

Regional Frequency Analysis of Extreme Precipitation with Consideration of Uncertainties to Update IDF Curves for the City of Trondheim

Hailegeorgis*, Teklu, T., Thorolfsson, Sveinn, T., and Alfredsen, Knut

Department of Hydraulic and Environmental Engineering, Norwegian University of Science and Technology (NTNU), N-7491 Trondheim, Norway

Summary Regional frequency analysis based on the method of L -moments is performed from annual maximum series of extreme precipitation intensity to update Intensity-Duration-Frequency (IDF) curves for the city of Trondheim. The main problems addressed are (1) reduction of uncertainties of different sources for reliable estimation of quantiles: (i) testing of trend patterns and stationarity of the data series from the target site and demonstrating the dependency of results on the data used; (ii) testing regional homogeneity of extreme precipitation events for the climate regime in the study area and “pooling” of regional data for data augmentation and reduction of uncertainty due to short length of data series; and (iii) selection of distributions for extreme precipitation events of different durations to reduce the uncertainty due to choice of distributions; and (2) assessment and quantification of sampling uncertainty in terms of interval estimates (confidence bounds) of quantiles. Trend patterns and check for stationarity have been demonstrated for a data from a target site based on both non-parametric Mann-Kendall and parametric regression tests. Selection of distributions has been done based on Z -statistics and L -moment ratio diagrams. Non-parametric balanced bootstrap resampling has been used to quantify the sampling uncertainty. For extreme precipitation events of shorter durations (5 min. to 30 min.) there are statistically significant increasing trend patterns for the data series with start years of 1992 to 1998 while there are no significant trend patterns for recent extremes and there are no statistically significant trend patterns for longer durations (45 min. to 180 min.). The results of the analyses indicate that: (1) significance tests for trend patterns and stationarity are dependent on the data series used but the stationarity assumption is valid for the data series used from the target site. (2) the extreme precipitation events from four sites in Trondheim are homogeneous and can be “pooled” for regional analysis; (3) different types of distributions fit to extreme precipitation events of different durations which shows that thorough selection of distributions is indispensable rather than fitting a single distribution for the whole durations; (4) interval estimates from balanced bootstrap resampling indicated that there is huge sampling uncertainty in quantile estimation that needs to be addressed in any frequency analysis; and (5) large differences are observed between the IDF curves from this study and the existing IDF curves (i.e. Imetno). The IDF

curves from this study are from data augmented through regional analysis, based on thorough procedures for selection of distributions and also include uncertainty bounds and hence are more reliable than the existing one. Hence, the methods and procedures followed in this study are expected to contribute to endeavors for estimating reliable IDF curves.

* Corresponding author. Tel.: [+47] 73592411; fax: [+47] 735 91298; E-mail addresses: teklu.hailegeorgis@ntnu.no, sveinn.thorolfsson@ntnu.no, knut.alfredsen@ntnu.no

1 **Corresponding author information:**

2 Name: Teklu Tesfaye Hailegeorgis

3 Address: S. P. Andersens veg 5, Hydraulic and Environmental Engineering, NTNU, N-7491
4 *Trondheim, Norway*

5 Tel. (office): [+47] 73592411

6 Cell phone: [+47] 45069384

7 Fax: [+47] 735 91298

8 E-mail addresses:

9 tekhi09@gmail.com

10 teklu.hailegeorgis@ntnu.no

11 Affiliations:

12 PhD Candidate at Norwegian University of Science and Technology (NTNU), Trondheim,
13 Norway: <http://www.ntnu.edu/employees/teklu.hailegeorgis>

14 Funded by CEDREN (Centre for Environmental Design of Renewable Energy):

15 <http://www.cedren.no/Projects/HydroPEAK.aspx> and working on Hydrology under Hydro-
16 PEAK projects:

17 <http://www.cedren.no/LinkClick.aspx?fileticket=b9CoekjEZQk%3D&tabid=3993>

18

19 **Keywords:**

20 Regional frequency analysis

21 L-moments

22 Extreme precipitation events

23 Intensity-Duration-Frequency curves

24 Uncertainties

25 Balanced bootstrap resampling

26 **1. Introduction**

27 Frequency analysis of extreme precipitation events of different durations have long been
28 used for the estimation of extreme quantiles corresponding to return periods of interest.
29 Estimated quantiles are summarized in the form of IDF curves from which design storm
30 hyetographs can be derived. The information is then useful for the design and management of
31 urban drainage infrastructure, bridges, spillways, risk analysis for landslide hazards, etc.

32 However, due to the prevalence of extreme precipitation events and vulnerability of urban
33 environments, urban floods have resulted in catastrophic damages in the recent years for
34 instance flooding in the city of Trondheim in August, 2007 (Thorolfsson et al., 2008). There is
35 growing interest from different stakeholders such as municipalities, companies, engineers, etc.
36 for reliable analysis of extreme precipitation events with uncertainty bounds and procedures
37 for routine updating. Therefore, reliable estimation of quantiles and derivation of design storm
38 hyetograph are required to reduce prediction uncertainty and hence to reduce the costs
39 associated with either spillover or over design.

40 For sites with sufficient record length as compared to the return period of the extreme
41 precipitation quantile of interest, at-site frequency analysis can be employed. But some sites
42 are not gaged at all or long historical records are not usually available to be able to make
43 reliable prediction of extreme quantiles for larger return periods. Hence data augmentation
44 from the regional observations is performed by utilizing extreme precipitation intensity
45 records in a region. This regional frequency analysis is based on delineation of hydrologically
46 homogeneous sites in the region and can also be useful to characterize the spatial relationships
47 of extreme precipitation events and to study the regional patterns of climatic variability or
48 change besides its main purpose of data augmentation.

49 Several studies (Adamowski et al., 1996; Gellens et al., 2002; Nguyen et al., 2002;
50 Fowler et al., 2003; Lee et al, 2003; Trefry et al., 2005; Wallis et al, 2007 and Norbiato et al.,
51 2007) have been done on regional frequency analysis of extreme precipitation or rainfall
52 events based on *L*-moments or updating of IDF curves for different parts of the world. Gaál et
53 al. (2008) applied region of influence (ROI) approach and *L*-moment based “index storm”
54 procedure for frequency analysis of heavy precipitation in Slovakia. Kyselý et al. (2007) have
55 derived the regional growth curves from regional frequency analysis based on *L*-moments for
56 improved estimates of design values and they have concluded that the regional approach is
57 most advantageous for variables such as precipitation that exhibit high random spatial

58 variability. Yang et al (2010) have analyzed rainfall extremes in the Pearl River basin in
59 China using *L*-moments augmented by tests for stationarity and correlation. Data pooling and
60 regionalization procedures which are based on the method of *L*-moments is widely employed
61 due to its rigorous statistical tests rather than simple approaches such as based on averaging
62 (for instance, Bengtsson and Milloti, 2010) of storm depths from at-site quantile estimations
63 from the stations in the region.

64 However, regional frequency analysis of extreme precipitation events and hence
65 derivation of IDF curves is subject to the major uncertainties of different sources which are
66 not addressed in the previous studies (see also Hailegeorgis and Burn, 2009):

- 67 a. Data series used: data quality, which is related to questions like is the data series
68 stationary and independent; and sampling of data, which are related to the time period and
69 length of data series and the sampling type (i.e. annual maximum series or partial duration
70 series which is peaks over thresholds);
- 71 b. Selection of frequency distribution;
- 72 c. Parameter estimation; and
- 73 d. Regionalization and quantile estimation

74 One of the main assumptions in the statistical frequency analysis from historical
75 (observed) data series is the stationarity assumption. However, there may be observed trends
76 in extreme precipitation events mainly due to anticipated climate change and hence there is
77 uncertainty involved with the stationarity assumption. The presence of significant non-
78 stationarity in hydrologic time series cannot be ignored when estimating design values for
79 future time horizons (Cunderlik and Burn, 2003). Bradley (1998) found that there is strong
80 evidence for climate-related non-randomness in extreme precipitation in the Southern plains
81 of the United States. Adamowski et al. (2003) detected significant trends in annual maxima
82 rainfall data for durations ranging from 5 minute to 12 hour for Ontario (Canada) using the
83 regional average Mann-Kendall. Crisci et al. (2002) have studied the uncertainties due to
84 trends connected with the estimation of the design storms for Tuscany (Italy) by Pearson
85 linear correlation coefficient and the Mann-Kendall tests. They have demonstrated that the
86 hydrological consequences of this kind of climate variability have a major impact on the
87 design of hydraulic works in the basin. However, there are still limitations in the commonly
88 used trend test procedures due to the dependency of their results on the data series used.

89 Long time series data is required for reliable analysis of trend and to substantiate whether
90 there is really a change or not for the long-term planning purposes. Therefore, analysis of such

91 type of trends is not an objective in here. But, an insight in to the patterns of trend and check
92 for stationarity of the historical data can also be pursued from the available relatively short
93 records in this type of analysis. Zhang et al. (2010) analyzed the pattern of trends of
94 streamflow based on different start and end years with a length of records from 10 years to 80
95 years. Bengtsson and Milloti (2010) have analyzed trends in hourly and sub-hourly annual
96 maximum precipitation of events of 25 years to 27 years long. Being data dependent analysis,
97 estimation of extreme events need to be updated regularly when new extremes data are
98 recorded in the region as regular update is indispensable for management and evaluation of
99 the performances of water infrastructure, for vulnerability and risk analysis, etc.

100 Annual maximum series rather than partial duration series (peaks over thresholds) method
101 of sampling of extreme precipitation have been used in this study. This avoids the uncertainty
102 related to subjective choice of the threshold values above which the extreme events are
103 included in the analysis. One may opt for comparing the results of regional frequency analysis
104 based on the *L*-moment from sampling based on annual maximum series vs. the peaks over
105 threshold type of sampling. But this task is not an objective of the present study.

106 Independence (i.e. no correlation) in the data series is also a main assumption in
107 frequency analysis. Correlation can be spatial correlation or serial correlation. Hosking and
108 Wallis (1997) noted that a small amount of serial dependence in annual data series has little
109 effect on the quality of quantile estimates. Data sampling based on the annual maximum
110 series which provides an additional advantage of avoiding the problem of serial correlation in
111 the data. Spatial correlation in data series as demonstrated by Hosking and Wallis (1988;
112 1997), Mikkelsen et al. (1996), Martins and Stedinger (2002), Madsen et al. (2002), Bayazit et
113 al. (2004), and Castellarin et al. (2008) can have an effect on the homogeneity test statistics
114 in regional frequency analysis. The effect of intersite dependence on the regional *L*-moment
115 algorithm is to increase the variability of the regional averages and this increases the
116 variability of estimated growth curve (Hosking and Wallis, 1997). Madsen et al. (2002), based
117 on partial duration series (PDS) of extreme rainfall analysis for Denmark, found that in
118 general the correlation is a decreasing function of distance and the correlation being larger for
119 larger durations. Also higher intersite correlation may be expected for low intensity (longer
120 duration) frontal storms which covers large areas than high intensity (shorter duration)
121 localized convective storms. The data used in this study from different sites in the region have
122 short concurrent records. Hence, intersite correlation in the data series is not a focus in this
123 study.

124 An additional challenge is that the results of frequency analysis from historical data are
125 dependent on the data series used. The length of the sample data may not be sufficient to
126 represent the underlying population especially for longer return periods, and there is no
127 general consensus on the guidelines regarding the required length of data series. For instance,
128 Jacob et al. (1999) suggested a 5T guideline that states “pooling” group should contain at least
129 5T station-years of data so as to obtain reasonably accurate estimates of the T-year quantile
130 while Mamen and Iden (2009), stated that one needs a series of at least 25 years to calculate
131 values for return period of 100 years. Hence, in general there is always uncertainty due to
132 sampling as different data series may result in different quantile estimates.

133 Selection of frequency distribution is also a major source of uncertainty in the estimation
134 of extreme quantiles as the sample data may reasonably fit to two or more distributions but
135 with significant differences in quantile values.

136 There are different methods of parameter estimation in frequency analysis which results
137 in different quantile estimates. The method of *L*-moments is used for parameter estimation in
138 this study due to its advantages mentioned by Hosking, 1990 such as *L*-moments being linear
139 functions of the data are less sensitive than are conventional moments to sampling variability
140 or measurement errors in the extreme data values and *L*-moment ratio estimators have small
141 bias and variance in comparison with the conventional moments. Hence uncertainty due to
142 parameter estimation is not dealt with in this study.

143 Also there is always uncertainty pertinent to delineation of homogeneous regions. Different
144 homogeneous regions can be delineated based on the criteria presented by Hoskings and
145 Wallis (1997) but may result in different estimated quantiles. Uncertainty due to
146 regionalization is not addressed in this study since it is not possible to form a big region for
147 the target site due to the availability of extreme precipitation data only at municipality level
148 which are many hundreds of kilometers apart and hence with a potentially heterogeneous
149 climate regime.

150 Furthermore, there is also uncertainty related to quantile estimation based on the “index
151 storm” procedure as use of different index values for instance the mean vs. the median values
152 may result in different quantile values. A middle-sized storm such as the mean or the median
153 can be used as an “index storm”. The difference between the mean and the median depends on
154 the skewness of the data fitted to a particular distribution. For instance, for a normal
155 distribution (i.e. zero skewness) the mean is equal to the median and both corresponds to the
156 50% probability of exceedence. Grover et al. (2002) have tested median flood as “index

157 flood". Also someone may be interested to test percentiles other than the mean and the
158 median. Nevertheless, investigation of the effect of choosing different "index storms" and its
159 pertinent uncertainty in the regional frequency analysis of extreme precipitation is not the
160 scope (objective) of this work. Plots of the "index storms" which are the mean of the annual
161 maximum series used in the present study are given in Fig. 5 while plots of the annual
162 maximum series are given in Fig. 6 to Fig. 9 for different durations of extreme precipitation
163 events for different sites considered in this study.

164 Therefore, the existing wide practice of frequency analysis and derivation of IDF curves
165 entails the following major limitations:

- 166 i. Only at-site frequency analysis based on short record length is widely applied which
167 makes quantile estimates of large return values less reliable;
- 168 ii. A single statistical distribution is fitted to extreme precipitations of different durations
169 without any thorough choice of the "best-fit" distribution which increases the uncertainty due
170 to the choice of distributions;
- 171 iii. There is no improved uncertainty bounds associated with the estimated quantiles hence
172 the end users are not able to propagate the uncertainty due to the IDF curves to the derivation
173 of IDF based design storm hyetographs and in the simulation of urban runoff (floods); and
- 174 iv. Lack of tests for trend patterns and stationarity in data series and lack of comprehensive
175 procedures which helps routine updating of the IDF curves.

176 **1.1. Objectives of the study**

177 The limitations which are stated above need to be addressed for improved predictions to
178 minimize the risks pertinent to the uncertainty in predictions. Hence the main objectives of
179 this study geared towards:

- 180 i. Application of procedures for trend patterns and stationarity tests in extreme precipitation
181 events of different durations for a target site to demonstrate the limitations in the existing
182 trend and stationarity test procedures due to their dependency on the data series used and
183 hence to assess the uncertainty pertinent to stationarity assumption;
- 184 ii. Detailed review of the derivations and procedures of regional frequency analysis of
185 extreme precipitation events based on the method of *L*-moments for better understanding of
186 the method. Estimation of *L*-moments directly from ordered observations and their
187 corresponding weights have been presented as a rather handy approach for implementation of

188 the method of *L*-moments and extension of the procedures and tools presented by Hosking
189 and Wallis (1997);
190 iii. Fitting the “best-fit” statistical distributions for each duration of extreme precipitation
191 events to reduce the uncertainty due to the choice of statistical distributions;
192 iv. Quantification of uncertainty in quantile estimation due to sampling of data series; and
193 v. Application of the methods to the climate regime in central Norway (i.e. city of
194 Trondheim) and updating of the IDF curves based on the regional analysis for the city.

195

196 **2. Study region and data**

197 The study site is the city of Trondheim, Norway. The city of Trondheim is chosen for the
198 study due to recent prevalence of extreme precipitation events (Thorolfsson et al., 2008),
199 growing interest by different stakeholders for better analysis of extreme precipitation events,
200 and relatively good records of regional data. Moreover, the availability of urban storm runoff
201 research catchment at Risvollan in the city gives the opportunity for further research related to
202 propagation of the uncertainties due to the IDF curves to design flood values. There is also a
203 plan to expand the regional methodology pertinent to data augmentation and prediction for
204 unengaged sites for other regions in Norway. But the importance of this work is not site and
205 problem specific that the methodologies and procedures developed or followed in this study
206 can be utilized elsewhere for similar objectives of analyzing extreme hydro-meteorological
207 events such as storms, floods, lowflows, wind speed, etc.

208 Extreme precipitation data is available for the period 1967 to 2009. Extreme precipitation
209 intensity data from four stations are “pooled” for regional analysis for this study (Table 1).
210 The mean annual precipitation from the existing metrological stations in the city ranges from
211 740 mm to 900 mm. Trondheim experiences extreme rainfalls during summer. It also
212 experiences precipitation in the form of snowfall during winter (from November to March).
213 The target site of Risvollan is located about 4 km southeast of the center of city of Trondheim
214 and have been an active urban research catchment since 1987 with separate storm sewer
215 networks of about 20 ha residential area. The site is equipped with instruments for measuring
216 precipitation, temperature, short wave solar radiation, wind velocity, relative humidity, snow
217 melt and storm water runoff (Matheussen, 2004). Owing to the availability of several
218 measurements, it is possible to execute further research for instance propagation of the
219 uncertainty in IDF curves to urban runoff simulation and analysis of flooding risks.

220

221 **3. Methodology**

222 **3.1. Trend pattern and stationarity**

223 Significance tests for trends are commonly used to detect the steady change (a trend) in
224 hydrologic time series before use for statistical analysis. Both non-parametric and parametric
225 methods are used to detect the significance of trends. The non-parametric test has made no
226 assumption about the statistical distributions of the data and hence they are not subject to the
227 uncertainty in the assumptions of the types of distributions. The parametric tests assume that
228 the time series data follows some particular distribution.

229 *Non-parametric test: Mann-Kendall test*

230 The non-parametric Mann-Kendall test (Mann, 1945; Kendall, 1975) is commonly used
231 for detection of direction of trend patterns in hydrological variables. The test procedures for
232 Mann-Kendall test have been described by many researchers for instance by Adamowski et al.
233 (2003) and McBean et al. (2008). For a time series of n data points where X_i and X_j are a
234 member of the data series where $i = 1, 2, \dots, n-1$ and $j = i+1, i+2, i+3, \dots, n$; each data point
235 X_i is compared with all corresponding X_j data points to compute the sign (i.e. direction of
236 trends). The Kendall's S-statistics is computed from the sum of the signs and the variance of
237 the S-statistics is computed. The null hypothesis to test (H_0) is there is no monotonic trend in
238 the data and the alternative hypothesis (H_1) is there is monotonic trend in the data. The test is
239 based on the Z-test. If $|Z_s| > (Z_{\alpha/2})$, we have an evidence to reject the null hypothesis
240 and hence that there is significant trend in the data where α is significance level. A
241 significance level of 5% i.e. a confidence level of 95% is used in this study.

242 *Parametric test: linear regression test*

243 In order to detect the trend, linear regression can be fitted between a response variable
244 which is the annual maximum series of precipitation intensity with the independent variable
245 which is the time (i.e. year) for different durations. The significance test is done for the slope
246 parameter of the linear regression model. Then from the statistical significance of the slope
247 parameter it can be inferred that there are trends in the annual time series data. The Null
248 hypothesis for trend test (H_0) is there is no significant trend and the alternative hypothesis
249 (H_1) is there is significant trend. The test is based on the t-test (see Rawlings et al, page 122).

250 The critical t-value is $t_{crit} = t_{\alpha/2, n-p}$. If $|t_{obs}| < t_{crit}$, we fail to reject the null hypothesis
 251 (i.e. no significant trend).

252 **3.2. Regional frequency analysis based on L-moments**

253 Frequency analysis of extreme precipitation events requires the availability of sufficient
 254 extreme precipitation data especially for reliable estimation of rare events (i.e. quantiles with
 255 large return periods). In regional frequency analysis, additional information from
 256 homogeneous sites within the region is utilized to improve the at-site estimates. Hosking and
 257 Wallis (1990; 1993; 1997), Burn (1988; 1990; 2003) and Martins and Stedinger (2002)
 258 demonstrated the importance of using regional information for frequency analysis of extreme
 259 hydrological events.

260 *L-moments and L-moment ratios*

261 Let X be a real-valued random variable with cumulative distribution $F(x)$, quantile
 262 function $x(F)$ and probability distribution function $f(x)$ or $dF(x)$. For a set of ordered data by
 263 $x_{1:n} \leq x_{2:n} \leq \dots \leq x_{n:n}$, certain linear combinations of the elements of an ordered sample
 264 contain information about the location, scale and shape of the distribution from which the
 265 sample is drawn hence L -moments are defined to be the expected values of these linear
 266 combinations, multiplied for numerical convenience by scalar constants (Hosking and Wallis,
 267 1997). The L -moments of a probability distribution are defined by (Hosking, 1990; Hosking
 268 and Wallis, 1997; Serfling and Xiao 2006, 2007)

269
$$\lambda_k = n^{-1} \sum_{r=1}^n w_{r:n}^{(k)} E[X_{r:n}] \tag{1}$$

270
$$w_{r:n}^{(k)} = \sum_{j=0}^{\min\{r-1, k-1\}} (-1)^{k-1-j} \binom{k-1}{j} \times \binom{k-1+j}{j} \binom{n-1}{j}^{-1} \binom{r-1}{j} \tag{2}$$

271 Where, $w_{r:n}^{(k)}$ are the weights and $r = 1, \dots, n$ are the ranks of the observations in ascending
 272 order. Hence the weights, which are the relative contributions of each observation to the first
 273 four L -moments for a sample size n are computed as:

274 $w_{r:n}^{(1)} = 1$

275 $w_{r:n}^{(2)} = \frac{2r - n - 1}{n - 1}$

276 $w_{rn}^{(3)} = \frac{(n-1)(n-2) + 6(r-1)(r-2) - 6(r-1)(n-2)}{(n-1)(n-2)}$

277 $w_{rn}^{(4)} = \frac{1}{(n-1)(n-2)(n-3)} \times \begin{cases} -(n-1)(n-2)(n-3) + \\ 20(r-1)(r-2)(r-3) + \\ 12(r-1)(n-2)(n-3) - \\ 30(r-1)(r-2)(n-3) \end{cases} \quad (3)$

278 L -moment ratios are independent of units of measurement and are given by Hosking and
 279 Wallis (1997) as follows:

280 $\tau = \frac{\lambda_2}{\lambda_1}, \tau_k = \frac{\lambda_k}{\lambda_2}; k \geq 3 \quad (4)$

281 Where, λ_1 is the L -location or the mean, λ_2 is the L -scale, τ is the L -CV, τ_3 is the L -skewness
 282 and τ_4 is the L -kurtosis.

283 *Estimators of L -moments and L -moment ratios*

284 Estimators of L -moments are obtained from finite sample. Hosking and Wallis (1997)
 285 (see formula 2.59 and Fig 2.6) have derived an expression for the sample L -moments (l_k)
 286 which are unbiased estimators of λ_k in terms of the ordered observations and their
 287 corresponding weights for the first four L -moments for a sample size of nineteen.

288 $l_k = n^{-1} \sum_{r=1}^n w_{r:n}^{(k)} x_{r:n}; k = 1, 2, \dots \quad (5)$

289 Where $w_{r:n}^{(k)}$ are the weights as defined in eqns. (2 and 3), $x_{r:n}$ are the ordered observations
 290 and $r = 1, 2, 3, \dots, n$ are the ranks of observations in ascending order. The first L -moment (λ_1)
 291 is the expectation or the mean of the distribution for a probability distribution and its
 292 estimator (l_1) is a sample mean and hence all the observations have equal weightages which
 293 are equal to one. Regional average L -moments are estimated from

294
$$l_k^R = \frac{\sum_{i=1}^N n_i \frac{l_k^{(i)}}{l_1^{(i)}}}{\sum_{i=1}^N n_i} ; k = 1, 2, \dots \quad (6)$$

295 Where, N is the total number of sites in the region, n_i is the number of records for each site
 296 and R denotes regional. Sample L -moment ratios t and t_k are natural estimators of τ and τ_k
 297 respectively and are not unbiased but their biases are very small in moderate or large samples

298 (Hosking and Wallis, 1997) and are defined as $t = \frac{l_2}{l_1}, t_k = \frac{l_k}{l_2}; k \geq 3 \quad (7)$

299 Implementation of eqns. (3 to 7) is not difficult. It can even be implemented as
 300 spreadsheet calculations so that it avoids relying mainly on previous work to apply the
 301 method of regional frequency analyses and also it encourages further extension or upgrading
 302 of the method with additional performances.

303 *Similarity measures and delineation of homogeneous regions*

304 Similar and homogeneous regions are identified and delineated based on specific
 305 similarity measures and homogeneity criterion respectively as proper delineation of
 306 homogeneous region is crucial for reliable quantile estimation. The region of influence
 307 approach (Burn, 1990, Zrinji and Burn, 1994) is used to identify similar sites and rank them
 308 based on their proximity to the target site as shown in Table 1. The attributes used for the
 309 similarity distance metrics have equal weights and include

- 310 a. Altitude of the stations;
- 311 b. Locations (X and Y co-ordinates of the stations); and
- 312 c. Mean annual precipitation at the stations

313 Hosking and Wallis (1997) presented the regional homogeneity based on the theory of L -
 314 moments which compares the regional dispersion of L -moment ratios with the average
 315 dispersion of the L -moment ratios determined from NS simulations of homogeneous groups
 316 from a four parameter Kappa distribution influenced only by sampling variability. Three
 317 heterogeneity measures are used to test the variability of three different H-statistics namely H_1
 318 for “coefficient of L -variation” (L -CV), H_2 for the combination of L -CV and L -skewness (L -
 319 SK) and H_3 for the combination of L -skewness (L -CS) and L -kurtosis (L -CK). Heterogeneity
 320 measures (H-statistics) are calculated as

321
$$H_i = \frac{V_{\text{observed}_i} - \mu_{V_{\text{simulated}_i}}}{\sigma_{V_{\text{simulated}_i}}}; i = 1, 2, 3$$
 (8)

322 Where $\mu_{V_{\text{simulated}_i}}$ and $\sigma_{V_{\text{simulated}_i}}$ are the means and standard deviations of the simulated
 323 values of dispersions (V_i) while V_{observed_i} are the regional dispersions calculated from the
 324 observations. The dispersions (V-statistics) are defined as

325
$$V_1 = \left\{ \frac{\sum_{i=1}^N n_i \left(t^{(i)} - t^R \right)^2}{\sum_{i=1}^N n_i} \right\}^{\frac{1}{2}}$$

326
$$V_2 = \frac{\sum_{i=1}^N n_i \left\{ \left(t^{(i)} - t^R \right)^2 + \left(t_3^{(i)} - t_3^R \right)^2 \right\}}{\sum_{i=1}^N n_i}$$

327
$$V_3 = \frac{\sum_{i=1}^N n_i \left\{ \left(t_3^{(i)} - t_3^R \right)^2 + \left(t_4^{(i)} - t_4^R \right)^2 \right\}}{\sum_{i=1}^N n_i}$$
 (9)

328
$$t^R = \frac{\sum_{i=1}^N n_i t^{(i)}}{\sum_{i=1}^N n_i}, t_k^R = \frac{\sum_{i=1}^N n_i t_k^{(i)}}{\sum_{i=1}^N n_i}; k \geq 3$$
 (10)

329 Where, V_1 is the standard deviation of the at-site sample L -CVs weighted based on record
 330 length. V_2 and V_3 are the weighted average distance from the site to the group weighted mean
 331 on graphs of t versus t_3 and of t_3 versus t_4 respectively, t^R , t_3^R and t_4^R are the regional average
 332 L -CV, L -SK, and L -CK respectively weighted proportionally to the sites' record length (n_i)
 333 and i represents the sites $1, 2, \dots, N$. Hosking and Wallis (1997) suggested that region can be
 334 regarded as “acceptably homogeneous” if $H < 1$, “possibly heterogeneous” if $1 \leq H < 2$, and
 335 “definitely heterogeneous” if $H \geq 2$.

336 *Discordancy measure*

337 A measure of discordancy between the L -moment ratios of a site and the average L -
 338 moment ratios of a group of similar sites identifies those sites that are discordant with the
 339 group as a whole and the procedures for discordancy measure as explained by Hosking and
 340 Wallis (1997) is as follows: Suppose there are N sites in the group, let $u_i = [t^{(i)} \ t_3^{(i)} \ t_4^{(i)}]^T$ be a
 341 vector containing the L -moment ratios t , t_3 and t_4 values for site i and the superscript T
 342 denotes transpose of a vector matrix, the group average \bar{u} and sample covariance matrix S are
 343 defined as

$$\begin{aligned} \bar{u} &= \frac{1}{N} \sum_{i=1}^N u_i \\ S &= \sum_{i=1}^N (u_i - \bar{u})(u_i - \bar{u})^T \end{aligned} \quad (11)$$

345 Then the discordancy measure D_i for a site is given by equation

$$D_i = \frac{1}{3} N (u_i - \bar{u})^T S^{-1} (u_i - \bar{u}) \quad (12)$$

347 A site should be declared discordant if $D_i \geq 3.0$.

348 *Selection of a regional frequency distribution (goodness-of-fit measure)*

349 The choice of frequency distributions is determined based on the goodness-of-fit
 350 measures which indicate how much the considered distributions fit the available data. It
 351 entails hypothesis tests to reject the null hypothesis which says a certain distribution fits to the
 352 data better than the other candidate distributions. If we fail to provide evidence to reject the
 353 null hypothesis the distribution is said to be the “best-fit”. Hosking and Wallis (1997) tested
 354 several distributions for the regional analysis and found that the two parameter distributions
 355 are not robust and vulnerable to “misspecification” and suggested that they are not
 356 recommended for regional or at-site analyses. Therefore, in the present study we considered
 357 the three parameter distributions which have also the shape parameters in addition to the scale
 358 and location parameters for the regional analyses. The analysis in the present study is based
 359 on historical records for which the stationarity assumption is tested to be valid. So, the
 360 methodology in the present study is different from the non-stationary extreme value analysis
 361 (such as Hundedcha et al., 2008; Mudersbach and Jensen, 2010, etc.) which considers an
 362 assumed time dependent patterns for some of the distribution parameters and also it is
 363 different from frequency analysis based on projected scenarios of extreme precipitation events

364 (such as Monette et.al., 2012, etc.). Therefore, when new extreme events are added to the
 365 analysis, the “best-fit” distribution, distribution parameters and also the quantile estimates and
 366 recurrence intervals may change which is the main limitation of any data dependent or data
 367 driven models.

368 However, the ultimate objective is estimation of more reliable and robust quantile values
 369 with uncertainty bounds from historical records (observations) which is expected to be a more
 370 reliable approach than the analyses based on the projected scenarios and non-stationary
 371 analysis. Quantile estimates from distributions which have shape parameters are expected to
 372 be robust and not highly sensitive to some new extreme precipitation events which are not
 373 included in the regional analysis. Therefore, selection of distributions also comply with the
 374 main essence of the regional analysis which include as much as possible extreme records in
 375 the region in to the data by “trading space for time” for data length augmentation and robust/
 376 reliable predictions at both gaged and ungaged sites. As it can be observed from Table 1, the
 377 regional extreme precipitation data is increased from 23 to 71 through pooling by the regional
 378 analysis based on the method of *L*-moments for the target site, Risvollan. When several
 379 distributions fit the data adequately, any of them is a reasonable choice for use in the final
 380 analysis, and the best choice from among them will be the distribution that is most robust
 381 (Hosking and Wallis, 1997). They proposed the five parameter Wakeby distribution as a
 382 default regional distribution if none of the considered candidate distributions fulfills the
 383 requirements of goodness-of-fit statistics.

384 The goodness-of-fit criteria defined in terms of *L*-moments for each of various
 385 candidate distributions are the *Z*-statistics and *L*-moment ratio diagram:

386 a. The *Z*- statistic

387 Fit a four parameter Kappa distribution to the regional average *L*-moment ratios t_1^R , t^R , t_3^R ,
 388 and t_4^R . Simulate a large number, N_{sim} , of realizations of a region with *N* sites, each from a
 389 four parameter Kappa distribution. For the m^{th} simulated region, calculate the regional
 390 average *L*-kurtosis $t_4^{[m]}$, the bias and standard deviation of t_4^R

$$391 \quad \beta_4 = \frac{1}{N_{sim}} \sum_{m=1}^{N_{sim}} \left(t_4^{[m]} - t_4^R \right)$$

$$392 \quad \sigma_4 = \left\{ \frac{1}{N_{sim} - 1} \left[\sum_{m=1}^{N_{sim}} \left(t_4^{(m)} - t_4^R \right)^2 - N_{sim} \beta_4^2 \right] \right\}^{\frac{1}{2}} \quad (13)$$

393 And, for each candidate distribution, the goodness-of-fit measure is given by

$$394 \quad Z^{DIST} = \frac{\tau_4^{DIST} - t_4^R + \beta_4}{\sigma_4} \quad (14)$$

395 Where, DIST refers to a particular distribution, β_4 and σ_4 are the bias and standard deviation
 396 of t_4^R respectively, N_{sim} is the number of simulated regional data sets in a similar way as for
 397 the heterogeneity statistics. The superscript m denotes the m^{th} simulated region. The fit is
 398 declared adequate if Z^{DIST} is sufficiently close to zero, a reasonable criterion being $|Z^{DIST}| \leq$
 399 1.64.

400 b. *L*-moment ratio diagram

401 Selection of the “best-fit” regional distribution using *L*-moment ratio diagrams involves
 402 plotting of the regional sample *L*-moment ratios (*L*-skewness vs. *L*-kurtosis) as a scatter plot
 403 and comparing them with theoretical *L*-moment ratio curves, which are given by Hosking and
 404 Wallis, 1997, of the candidate distributions. The distribution to which the regional *L*-moment
 405 ratios computed from the sample are closer to the theoretical curve is selected as the “best-
 406 fit”.

407

408 *Estimation of parameters and quantiles*

409 The main objective of frequency analysis is estimation of quantiles corresponding to a
 410 return period of interest. The parameters of distributions given in Appendix B are estimated
 411 from their relationship with *L*-moments and *L*-moment ratios as given by Hosking and Wallis
 412 (1997). Then the quantiles are estimated from quantile functions which are given in Appendix
 413 A. The “index storm” approach which is a similar approach to the index flood (Dalrymple,
 414 1960) is used for quantile estimation of extreme precipitation events. The main assumption of
 415 an “index storm” procedure is that the sites forming a homogeneous region have identical
 416 frequency distribution called the regional growth curve but a site-specific scaling factor, the
 417 “index storm”. Let $x(F)$, $0 < F < 1$, be the quantile function of the frequency distribution of
 418 extreme precipitation intensity at site i , for a homogeneous region

$$419 \quad x_i(F) = \mu_i q(F) \quad (15)$$

420 Where $i = 1, 2, \dots, N$ and μ_i is the site-dependent scale factor which is called the “index storm”
 421 and $q(F)$ is the regional growth curve which is a dimensionless quantile function common to
 422 every site in a homogeneous region.

423 Following previous work (Hosking and Wallis, 1997, Nguyen et al., 2002, Gaál et al.,
424 2008, etc.), the location estimator (i.e. the sample mean) of annual maximum series of
425 extreme precipitation intensity is used as an “index storm” in this study. More detailed
426 references on regional frequency analysis based on L -moments can be obtained from Hosking
427 and Wallis (1997).

428 **3.3. Balanced bootstrap resampling**

429 Quantile estimate from a single data set in regional frequency analysis provides only a
430 point estimate. Therefore, non-parametric balanced bootstrap resampling, which involves
431 random sampling with replacement, is employed to quantify sampling uncertainty in terms of
432 interval estimates (i.e. confidence intervals of quantile estimates). In bootstrap (Efron 1979;
433 1982), the samples are drawn with replacement from the original sample. Davison et al.
434 (1986) presented balanced bootstrap resampling which reuses each of the observations equal
435 number of times. In balanced bootstrap resampling, the total number of occurrences of each
436 sample point in the whole resamples is the same and is equal to the number of resampling
437 ($N_{\text{resampling}}$). Faulkner et al. (1999) derived confidence limits for growth curves of rainfall data
438 by bootstrapping. Burn (2003) applied bootstrap resampling for flood frequency analysis and
439 presented the main advantages of bootstrap resampling for constructing confidence intervals.
440 Also the initial spatial correlation of the data from different sites is not affected in bootstrap
441 resampling approach (Pujol et al., 2007).

442 In bootstrap, let the original sample data is $X = \{X_1, X_2, \dots, X_n\}$ and the bootstrap
443 resample of X is $X^* = \{X_1^*, X_2^*, \dots, X_n^*\}$, the estimators such as confidence intervals can then
444 be estimated from the resamples $(X^*)^{(1)}, (X^*)^{(2)}, \dots, (X^*)^{(N_{\text{resampling}})}$ of size $N_{\text{resampling}}$. The
445 background and method of estimating the confidence intervals as presented by Faulkner and
446 Jones (1999) and Carpenter (1999) is as follows: let Q_i is the estimate from the bootstrap
447 sample i , Q_{sam} is the estimate from sample data and Q_{true} is the unknown true quantity,
448 bootstrap residuals $e_i = Q_i - Q_{\text{sam}}$ and the actual unknown residual $e = Q_{\text{sam}} - Q_{\text{true}}$.
449 Assuming that bootstrap residuals (e_i) to be representative of values drawn from the same
450 distribution as the actual unknown residual (e), $Q_i - Q_{\text{sam}} \equiv Q_{\text{sam}} - Q_{\text{true}}$. If e_l and e_u are
451 appropriate lower and upper percentage points of the unknown distribution of the residuals,
452 such that the probability

$$\Pr(e_l \leq e \leq e_u) = 1 - 2\alpha \rightarrow$$

$$453 \quad \Pr(e_l \leq Q_{sam} - Q_{true} \leq e_u) = 1 - 2\alpha \rightarrow$$

$$\Pr(Q_{sam} - e_u \leq Q_{true} \leq Q_{sam} - e_l) = 1 - 2\alpha$$

$$454 \quad \text{Then, } (LCL, UCL) = (Q_{sam} - e_u, Q_{sam} - e_l) \quad (16)$$

455 e is equally likely to appear at any point in the ordered set of e_i 's, i.e. each has a probability of

$$456 \quad \frac{1}{(N_{resampling} + 1)}.$$

457 Then, $u = \alpha \times (N_{resampling} + 1)$ and

$$458 \quad l = (1 - \alpha) \times (N_{resampling} + 1) \quad (17)$$

459 Where, $\alpha = 1/2$ of the significance level.

460 The procedures for balanced bootstrap resampling based on regional L -moment parameter
461 estimation algorithm to construct $100(1-2\alpha)$ % confidence intervals of quantile estimates,
462 following Faulkner and Jones (1999), Burn (2003) and Hailegeorgis and Burn (2009) is given
463 as below:

- 464 i. Prepare original sample “pooled” from homogeneous region;
- 465 ii. By repeating each year of data $N_{resampling}$ times we would get a matrix of
466 $(N_{years} * N_{resampling})$ rows by N_{sites} columns, where N_{years} is the number of years for which data
467 is available at one or more data stations and N_{sites} is the number of homogeneous sites for
468 regional analysis;
- 469 iii. Balanced bootstrap resamples are then obtained from random permutation of N_{years} rows
470 of data from which L -moments, L -moment ratios, parameters and quantiles corresponding to a
471 return period of interest can be estimated for the selected “best-fit” distributions given in
472 Table 2. This process is then repeated $N_{resampling}$ times;
- 473 iv. Calculate bootstrapped residuals (e_i), which are the deviations of each quantile estimates
474 from the quantile estimate of the original sample. $e_i = Q_i - Q_{sam}$, where Q_i is quantiles
475 estimated from bootstrapped samples and Q_{sam} is quantile estimated from the original sample;

476 v. Rank these deviations in ascending order to find e_u and e_l for 95% confidence interval
477 where u and l are defined as above and correspond to the upper and the lower confidence
478 levels respectively. For $N_{\text{resampling}} = 999$ used in this study, u corresponds to 25th and l
479 corresponds to 975th bootstrap residuals; and
480 vi. Finally, the confidence intervals for the estimated quantiles are computed from (16).

481

482 **4. Results**

483 Since the annual maximum precipitation intensity data series from the other sites
484 considered are short and/or don't include recent extremes (Table 1), only the data series for
485 the target site of Risvollan has been tested for trend patterns and stationarity to check the
486 validity of stationarity assumption and to demonstrate the dependency of trend patterns on the
487 data series used. In this study, the method by Zhang et al. (2010) is adopted and a trend test
488 based on varying starting period and fixed end period is used. Both the parametric Mann-
489 Kendall and the non-parametric regression tests have produced similar results for trend
490 patterns. For the target site, the data used for the analysis of extreme precipitation can be said
491 to be stationary (Fig. 2 and 3) and hence stationary frequency analysis is valid.

492 For this study, no site has appeared to be discordant based on the discordancy measure
493 explained earlier. Results of homogeneity tests based on H-statistics (Table 2) indicated that
494 H-values range from -1.75 to 1.22.

495 Results for the selection of statistical distribution are given in Table 2 and Fig. 4. Four
496 different types of three parameter distributions, the Generalised extreme value (GEV),
497 Generalised logistic (GLO), Pearson Type III (PIII) and Generalized Pareto (GPAR) are
498 tested. Different types of statistical distributions appeared to be the "best-fit" for extreme
499 precipitation of different durations. The "best-fit" distribution for precipitation durations of 5
500 min., 45min. and 120 min. is the Pearson Type III; Generalised Pareto distribution is the
501 "best-fit" and also the only fit for extreme precipitation of 10 min., 20 min. and 30 min.
502 durations. Generalised logistic distribution is the "best-fit" distribution for extreme
503 precipitations of 60 min., 90 min. and 180 min. durations. Identification of distribution based
504 on a regional L -moment ratio diagram (Fig. 4) also resulted in similar "best-fit" distributions
505 as that of the Z -statistics for all durations of extreme precipitation events. IDF curves with
506 uncertainty bounds (95 % confidence intervals) for the target site are given in Fig. 10 and 11.

507 Percentage differences of the 95% lower and upper confidence levels of quantiles (which are
508 estimated based on bootstrap resampling) and the existing IDF curve (i.e. estimated from at-
509 site analysis for the target site of Risvollan by the Metrological Institute of Norway:
510 www.eklima.no and labeled as Imetno in Fig. 10 and 11), from the quantiles estimated from
511 regional analysis in this study are given in Table 3. The differences in quantile estimates from
512 this study as revealed from the 95% confidence bounds range from -32.9 % to +25.1 % for a
513 return period of 2 years and rises to -43 % to +31% for a return period of 100 years. The
514 percentage differences in the existing IDF quantiles and the quantiles estimated from this
515 regional analysis ranges from +25.8 % for a return period of 2 years to - 40 % for a return
516 period of 100 years.

517

518 **5. Discussion**

519 *Trend pattern and stationarity*

520 The varying starting periods used for trend tests help to identify the start year of
521 significant trend patterns. The fixed end period is used since the objective is to assess the
522 patterns of the trend for recent extremes to detect the recent trends and to utilize the updated
523 information for design and management. It can be indicated that different results for
524 significant test for trends are obtained from data set from varying starting years until recent
525 extremes. But the extreme precipitation data set used for the target site for regional frequency
526 analysis covers from 1987 to 2009 and trend patterns vanish for the data series containing
527 recent extremes (Fig. 2 and 3). Therefore, based on the analysis of data series from the target
528 site, stationarity assumption is valid and *L*-moments based frequency analysis can reasonably
529 be applied.

530 *Discordancy test and homogeneity tests based on H-statistics*

531 All the H-values are less than one for durations of 5 min. to 120 min. which shows that
532 the region is “acceptably homogeneous” and the H-value is slightly greater than one and less
533 than two ($H_1 = 1.22$) for duration of 180 min. which shows that the region is “ possibly
534 heterogeneous”. Therefore, the data used from the study region can be ”pooled” based on the
535 criterion presented by Hosking and Wallis (1997) for data augmentation and hence reliable
536 estimation of quantiles. This study subsatntiates that it is worth testing the homogeneity of
537 extreme precipitation from a further wide spatial extent for the climate regime in Norway for
538 reliable estimation of quantiles of high return periods and also for estimation of regional IDF

539 curves or regional quantile maps to be able to estimate the design values at ungaged locations
540 in the region.

541 *Selection of distributions based on Z-statistics and L-moment diagram*

542 It can be indicated that two or more distributions ($Z \leq 1.64$) may fit the extreme
543 precipitation data but the “best-fit” distribution for which the quantile is estimated is the one
544 with Z-value closer to Zero. Therefore, it is indicated that it is very important to follow
545 thorough statistical distributions selection procedures rather than fitting a single distribution
546 for all extreme precipitations of different durations in order to reduce the uncertainty in
547 quantile estimation pertinent to the selection of the “best-fit” statistical distribution for the
548 extreme data considered.

549 *Quantile estimations and uncertainty bounds*

550 From the confidence bounds of estimated quantiles, it can be observed that there is large
551 sampling uncertainty which increases with the return period. These uncertainty ranges have
552 inevitable impact on the design magnitudes of urban drainage infrastructure. The existing IDF
553 curves for the city of Trondheim is based on at-site fitting of the two parameter extreme value
554 Type I (EV1) or Gumbel distribution for the whole durations of extreme precipitation events.
555 The EV1 (Gumbel) distribution is the special case of the Generalised extreme value (GEV)
556 distribution when the shape parameter is zero ($k = 0$). But the tail behavior of a distribution
557 is largely influenced by its shape parameter(s). In the contrary reliable prediction of the rare
558 extreme quantiles of higher recurrence intervals, which are located at the tails of a distribution
559 are of main interest to minimize the risks pertinent to the occurrence of extreme events.
560 Despite its drawbacks, the Gumbel distribution is usually appealing to hydrology practitioners
561 and for teaching purposes due to its simplicity in parameter estimation by the method of
562 moments, method of maximum likelihood, and L-moments.

563 The same at-site data for Risvollan as the present study was used by the Norwegian
564 Meteorological Institute to develop the existing IDF curves. The improvement obtained from
565 the present work is due to the regional analysis based on the use of regional records rather
566 than the at-site estimation from records of short length (i.e. at-site analysis). Plots of the
567 existing IDF curves (Fig. 10 and 11) reveal that there is a sharp bend in the IDF curves above
568 duration of 20 minutes which indicates that the statistical distribution fitted to the extreme
569 precipitation of above 20 min. durations may not represent the parent distribution (i.e. there is
570 “misspecification” of statistical distribution). In addition, the fitted two parameter distribution

571 which has no shape parameter lacks robustness and hence “misspecification” of distribution
572 affects the quantile estimation to a larger extent.

573 **6. Conclusions**

574 Regional frequency analysis of extreme precipitation events based on the method of *L*-
575 moments has been reviewed and applied for the city of Trondheim for data augmentation and
576 reliable estimation of quantiles. Extreme precipitation intensities of durations 5 min. to 180
577 min., which can be relevant for design and management of urban water infrastructure, are
578 “pooled” from four gaging stations in the city of Trondheim for regional frequency analysis
579 and estimation of quantiles corresponding to 2 to 100 years return period. *L*-moments are
580 estimated directly from ranked and weighted ordered sample data series which is a
581 contribution towards further understanding of the *L*-moment procedures of regional frequency
582 analysis. The approach is not difficult and it helps for easy implementation of the *L*-moment
583 procedures especially for extension with additional developments such as assessment of
584 uncertainty as demonstrated in this study.

585 Check for stationarity of data and the dependency of the commonly used trend test procedures
586 on the sample data used has been demonstrated and thorough trend pattern tests based on data
587 from varying start years and also that include recent extremes should be followed and general
588 conclusion on the stationarity of the data need to be drawn with caution.

589 It can be indicated that different statistical distributions fit to extreme precipitation events
590 of different durations and hence careful choice of “best-fit” and robust statistical distributions
591 for different durations is indispensable to reduce the uncertainty pertinent to selection of
592 distributions.

593 The sampling uncertainty associated with the frequency analysis of extreme precipitation
594 events is assessed and quantified in terms of interval estimate (i.e. 95% confidence bounds)
595 based on non-parametric bootstrap resampling. The interval estimate showed that there is
596 huge uncertainty in quantile estimation due to sampling of data which needs to be
597 incorporated in any frequency analysis from historical data. The updated estimated quantiles
598 and IDF curves with uncertainty bounds obtained from this study are found to be more
599 reliable as compared to the existing IDF curves for Trondheim.

600 The methods and procedures followed in this study are expected to contribute to
601 endeavors for estimating reliable quantiles and reducing the uncertainties associated with IDF

602 curves. IDF curves with quantified uncertainty bounds would help the end users to be able to
603 recognize the uncertainties behind the IDF curves and propagate the uncertainties pertinent to
604 IDF curves for reliable derivation of IDF curves based design storm hyetographs and
605 simulation of urban runoff in the design and management of urban drainage infrastructure or
606 in any flood risk assessment tasks.

607 This study focuses on the assessment and quantification of sampling uncertainty pertinent
608 to IDF curves and hence it can't be considered as a comprehensive uncertainty assessment.
609 Also propagation of this uncertainty to simulation of urban runoff is not studied. This task is
610 planned for future research.

611

612 **Acknowledgments**

613 The first author is substantially funded by CEDREN (Centre for Environmental Design of
614 Renewable Energy: <http://www.cedren.no/>). We would like to acknowledge Knut A. Iden and
615 Hanna Szewczyk-Bartnicka of the Norwegian Meteorological Institute for providing the
616 extreme precipitation data which is used in this study. Also, we wish to acknowledge the two
617 anonymous reviewers for their detailed review and helpful comments to improve the
618 manuscript.

619

620 **References**

- 621 Adamowski, K., Alila, Y., and Pilon, P.J. (1996). Regional rainfall distribution for Canada.
622 Atmos. Res. 42, 75-88.
- 623 Adamowski, K., and Bougadis, J. (2003). Detection of trends in annual extreme rainfall,
624 Hydrological Processes, 17(18), 3547-3560.
- 625 Bayazit, M. and Önöz, B. (2004). Sampling variances of regional flood quantiles affected by
626 intersite correlation. Journal of Hydrology, 291, 42-51.
- 627 Bengtsson, L., and Milloti, S. (2010). Extreme storms in Malmö, Sweden. Hydrological
628 Processes, 24, 3462-3475.
- 629 Bradley, A.A. (1998). Regional frequency analysis method for evaluating changes in
630 hydrological extremes. Water Resources Research, 34(4), 741-750.
- 631 Burn, D. H. (1988). Delineation of groups for regional flood frequency analysis. Journal of
632 Hydrology, 104(1-4), 345-361.

633 Burn, D. H. (1990). Evaluation of regional flood frequency analysis with a region of influence
634 approach. *Water Resources Research*, 26(10), 2257-2265.

635 Burn, D. H. (2003). The use of resampling for estimating confidence intervals for single site
636 and pooled frequency analysis. *Hydrological Sciences Journal*, 48(1), 25-38.

637 Burn, D. H., and Goel, N. K. (2000). The formation of groups for regional flood frequency
638 analysis. *Hydrological Sciences Journal*, 45 (1), 97-112.

639 Carpenter, J. (1999). Test inversion bootstrap confidence intervals. *Journal of the Royal*
640 *Statistical Society (Series B): Statistical Methodology*, 61(1), 159-172.

641 Castellarin, A., Burn, D. H., and Brath, A. (2008). Homogeneity testing: How homogeneous
642 do heterogeneous cross-correlated regions seem?. *Journal of Hydrology*, 360(1-4), pp. 67-76.

643 Crisci, A., Gozzini, B., Meneguzzo, F., Pagliara, S., and Maracchi, G. (2002). Extreme
644 rainfall in a changing climate: Regional analysis and hydrological implications in Tuscany,
645 *Hydrological Processes* 16, 1261-1274.

646 Cunderlik, J.M., and Burn, D.H. (2003). Non-stationary pooled flood frequency analysis.
647 *Journal of Hydrology* 276, 210-223.

648 Darlymple, T. (1960). Flood frequency analysis. Rep. No. Water supply paper 1543-A,
649 U.S.Geological Survey, Reston, VA, U.S.

650 Davison, A.C., Hinkley, D.V., and Schechtman, E. (1986). Efficient Bootstrap Simulation.
651 *Biometrika*, 73(3), 555-566.

652 Efron, B. (1979). Bootstrap methods: another look at the jackknife. *The Annals of Statistics* 7
653 (1): 1-26.

654 Efron, B. (1982). The jackknife, the bootstrap, and other resampling plans. Society for
655 Industrial and Applied Mathematics, Philadelphia, Pa.

656 Faulkner, D. S., and Jones, D. A. (1999). The FORGEX method of rainfall growth estimation;
657 III, examples and confidence intervals. *Hydrology and Earth System Sciences (HESS)*, 3(2),
658 205-212.

659 Fowler, H. J., and Kilsby, C. G. (2003). A regional frequency analysis of United Kingdom
660 extreme rainfall from 1961 to 2000. *International Journal of Climatology*, 23(11), 1313-1334.

661 Gaál, L., Kysely, J., and Szolgay, J. (2008). Region-of-influence approach to a frequency
662 analysis of heavy precipitation in Slovakia. *Hydrology and Earth System Sciences*, 12(3),
663 825-839.

664 Gellens, D. (2002). Combining regional approach and data extension procedure for assessing
665 GEV distribution and extreme precipitation in Belgium, *Journal of Hydrology*, 268, 113-126.

666 Gilchrist, W. G. (2000). Statistical modeling with quantile functions. CHAPMAN and

667 HALL/CRC.

668 Greenwood, J. A., Landwehr, J. M., Matalas, N. C., and Wallis, J. R. (1979). Probability
669 weighted moments: definition and relation to parameters of several distributions expressible
670 in inverse form. *Water Resources Research*, 15, 1049-1054.

671 Grover, Patrick L., Burn, Donald H., and Cunderlik, Juraj M. (2002). A comparison of index
672 flood estimation procedures for ungauged catchments. *Can. J. Civ. Eng.* 29, 734–741.

673 Guo, Y. (2006). Updating rainfall IDF relationships to maintain urban drainage design
674 standards. *Journal of Hydrologic Engineering*, 11(5), 506-509.

675 Hailegeorgis, Teklu. T, and Burn, D. H. (2009). Uncertainty assessment of the impacts of
676 climate change on extreme precipitation events. A report prepared for the Canadian
677 Foundation for Climate and Atmospheric Sciences (accessed on July 10/2011). Available at
678 [http://www.eng.uwo.ca/research/iclr/fids/publications/cfcas-](http://www.eng.uwo.ca/research/iclr/fids/publications/cfcas-quantifying_uncertainty/Reports/Teklu_report.pdf)
679 [quantifying_uncertainty/Reports/Teklu_report.pdf](http://www.eng.uwo.ca/research/iclr/fids/publications/cfcas-quantifying_uncertainty/Reports/Teklu_report.pdf).

680 Hosking, J.R.M. (1988). FORTRAN Routines for use with the Method of L-Moments, IBM
681 Research Division, T. J. Watson Research center, Yorktown heights, New York 10598,
682 U.S.A., July 1988.

683 Hosking, J.R.M. (1990). L-Moments: Analysis and estimation of distributions using linear
684 combinations of order statistics. *Journal of Royal Statistical Society. Series B*
685 (*Methodologica*), 52 (1), 105-124.

686 Hosking, J. R. M. and Wallis, J. R. (1988). The effect of intersite dependence on regional
687 flood frequency analysis. *Water Resources Research*, 24, 588-600.

688 Hosking, J.R.M. and Wallis, J. R. (1993). Some Statistics useful in regional frequency
689 analysis. *Wat. Resour. Res.* 29 (2), 271-281.

690 Hosking, J. R. M. and Wallis, J. R. (1997). *Regional Frequency Analysis: An Approach*
691 *Based on L-Moments*, © Cambridge University Press, New York, NY, 224 pages.

692 Hosking, J. R. M. and Wallis, J. R., Wood, E. F. (1985). Estimation of the generalized
693 extreme-value distribution by the method of probability weighted moments. *Technometrics*,
694 27, 251-261.

695 Hundecha, Y., St -Hilaire, A., Ouarda, T.B.M.J., and El adlouni, S. (2008). A Nonstationary
696 Extreme Value Analysis for the Assessment of Changes in Extreme Annual Wind Speed over
697 the Gulf of St. Lawrence, Canada. *Journal of applied meteorology and climatology*, 47, 2745-
698 2759.

699 Jacob, D., Reed, D. W., and Robson, A. J. (1999). Choosing a pooling group. *Flood*
700 *Estimation Handbook*, Institute of Hydrology, Wallingford, U.K.

701 Kendall, M.G. (1975). Rank correlation measures. Charles Griffin, London.

702 Kysely, J., and Picek, J. (2007). Regional growth curves and improved design value estimates
703 of extreme precipitation events in the Czech Republic. *Climate Research*, 33(3), 243-255.

704 Lee, S.H. and Maeng, S.J. (2003). Frequency analysis of extreme rainfall using L-moment..
705 *Irrigation and Drainage*, 52 (3), 219-230.

706 Madsen, H., Mikkelsen, P.S., Rosbjerg, D., Harremoës, P. (2002). Regional estimation of
707 rainfall intensity-duration-frequency curves using generalized least squares regression of
708 partial duration series statistics. *Water Resources Research* 38 (11), 1239.

709 Mamen, J. and Iden, K. A. (2009). Analyse Av korttidsnedbør i Norge 1967-2009. met.no
710 report no. 11/2010. Climate. Norwegian Meteorological Institute.

711 Mann, H.B. (1945). Non-parametric tests against trend. *Econometrica*, 13 (3), 245-259.

712 Markus, M., Angel, J. R., Yang, L., and Hejazi, M. I. (2007). Changing estimates of design
713 precipitation in northeastern Illinois: Comparison between different sources and sensitivity
714 analysis. *Journal of Hydrology*, 347(1-2), 211-222.

715 Martins, E.S., and J.R. Stedinger (2002). Cross correlations among estimators of shape. *Water*
716 *Resources Research* 38 (11), 1252.

717 Mathuesen, B.V.(2004). Effects of anthropogenic activities on snow distribution, and melt in
718 an urban environment. PhD. Dissertation. Faculty of Engineering Science and Technology.
719 Norwegian University of Science and Technology.

720 McBean, E. and Motiee, H. (2008). Assessment of impact of climate change on water
721 resources: a long term analysis of the Great Lakes of North America, *Hydrol. Earth Syst. Sci.*,
722 12, 239-255.

723 Mikkelsen, P.S., and Harremoës, P. (1993). Uncertainties in urban runoff extreme value
724 calculations caused by statistical/geographical variation in rainfall data, in *Proceedings of*
725 *Sixth International Conference on Urban Storm Drainage*, 1, edited by J. Marsalák and H.
726 Tomo, 471-476, Seapoint, Victoria, British Columbia, Canada.

727 Mikkelsen, P. S., Madsen, H., Rosbjerg, D., and Harremoës, P. (1996). Properties of extreme
728 point rainfall III: Identification of spatial inter-site correlation structure. *Atmospheric*
729 *Research*, 40(1), pp. 77-98.

730 Monette, A., Sushama, L., Khaliq, M.N., Laprise, R., and Roy, R. (2012). Projected changes
731 to precipitation extremes for northeast Canadian watersheds using a multi-RCM ensemble.
732 *Journal of geophysical Research*, 117, D13106, doi:10.1029/2012JD017543.

733 Mudersbach, C., and Jensen, J. (2010). Nonstationary extreme value analysis of annual
734 maximum water levels for designing coastal structures on the German North Sea coastline.

735 Journal of Flood Risk Management 3(1), 52–62.

736 Norbiato, D., Borga, M., Sangati, M. and Zanon, F. (2007). Regional frequency analysis of
737 extreme precipitation in the eastern Italian Alps and the August 29, 2003 flash flood. Journal
738 of hydrology, 345 (3-4), 149-166.

739 Nguyen, V. -T.-V., Nguyen, T. D., and Ashkar, F. (2002). In Burlando P. (Ed.), Regional
740 frequency analysis of extreme rainfalls. Pergamon, P.O. Box 800 Kidlington Oxford OX5
741 1DX UK: Elsevier Science Ltd.

742 Peel, M. C., Wang, Q.J., Vogel, R.M., and McMahon, T.A. (2001). The utility of L-moment
743 ratio diagrams for selecting a regional probability distribution. Hydrological Sciences 46 (1),
744 147-155.

745 Pujol, N., Neppel, L. and Sabatier, R. (2007). Regional tests for trend detection in maximum
746 precipitation series in the French Mediterranean region. Hydrological Sciences Journal, 52
747 (5), 956-973.

748 Rawlings, O., Sastry G. Pentula, David A. Dickey (1998). Applied regression analysis: A
749 research tool. 2nd ed. Springer texts in statistics.

750 Schaefer, M.G. (1990). Regional analyses of precipitation annual maxima in Washington
751 State, Water Resources Research, 26 (1), 119-131.

752 Serfling, R., and Xiao, P. (2006). A contribution to Multivariate L-moments: L-Comment
753 matrices. Department of Mathematical Sciences, University of Texas at Dallas. Full
754 unabridged version (accessed on Dec. 04/2010). Available at www.utdallas.edu/~serfling.

755 Serfling, R., and Xiao, P. (2007). A contribution to multivariate L-moments: L-comoment
756 matrices. Journal of Multivariate Analysis, 98(9), pp. 1765-1781.

757 Shao, Q., Hao, Z.C., Chen, X., Zhang Z.X., Xu, C.Y. Sun, L. (2010). Regional frequency
758 analysis and spatio-temporal pattern characterization of rainfall extremes in the Pearl River
759 Basin, China. Journal of Hydrology, 380 (3-4), 386-405.

760 Thorolfsson, S. T., Rishot, L. P., Nilsen, O., Ellingsson, A., Kristiansen, V., Hagen, Ø.,
761 Karlsen, E. (2008). Extreme rainfalls and damages on August 13 2007 in the City of
762 Trondheim, Norway. The XXV Nordic Hydrological Conference Northern Hydrology and its
763 Global role. Reykjavik, Iceland.

764 Trefry, C.M., David, W., Watkins Jr., and Johnson, D. (2005). Regional Rainfall Frequency
765 Analysis for the State of Michigan. Journal of Hydrologic Engineering, 10 (6), 437-449.

766 Wallis, J.R., Schaefer, M.G., Barker, B.L. and Taylor, G.H. (2007). Regional precipitation-
767 frequency analysis and spatial mapping for 24-hour and 2- hour durations for Washington
768 State. Hydrology and Earth System Sciences (HESS), 11 (1), 415-442.

769 Young, C. B., and McEnroe, B. M. (2006). Updated precipitation frequency estimates for
770 Kansas City: Comparison with TP-40 and HYDRO-35. *Journal of Hydrologic Engineering*,
771 11(3), 206-213.
772 Zhang, Z., Dehoff, A. D. and. Pody, R. D. (2010). New Approach to Identify Trend Pattern of
773 Streamflows. *Journal of Hydrologic Engineering*, 15 (3), 244-248.

774

775 **Appendices**

776

777 **Figure captions**

778 Fig. 1. Locations of precipitation stations used for regional analysis

779 Fig. 2. Results of Mann-Kendal and regression methods for trend pattern at 95 % confidence
780 intervals and check for stationarity for extreme precipitation of 5 min. to 30 min. durations at
781 Risvollan site (Trondheim) for different data start years to data end year of 2009

782 Fig. 3. Results of Mann-Kendal and regression methods for trend pattern at 95 % confidence
783 intervals and check for stationarity for extreme precipitation of 45 min. to 180 min. durations
784 at Risvollan site (Trondheim) for different data start years to data end year of 2009

785 Fig. 4. Regional L-Moment ratio diagram for identification of “best-fit” regional distributions

786 Fig. 5. Mean of annual maximum precipitation intensity or “index storm” used (1 l/s.ha or 1
787 liter/second.hectar = 0.36 mm/hr or 0.36 millimeter/hour

788 Fig. 6. Annual maximum precipitation series for different durations at Risvollan site

789 Fig. 7. Annual maximum precipitation series for different durations at Moholt-Voll site
790 (jumped years are missing data)

791 Fig. 8. Annual maximum precipitation series for different durations at Blakli site

792 Fig. 9. Annual maximum precipitation series for different durations at Tyholt site

793 Fig. 10. IDF curves and 95 % confidence intervals for Risvollan site (Trondheim) for quantile
794 estimates of 2, 5 and 10 years return periods from regional frequency analysis of annual
795 maximum extreme precipitation events of 5 min. to 180 min. durations

796 Fig. 11. IDF curves and 95 % confidence intervals for Risvollan site (Trondheim) for quantile
797 estimates of 20, 50 and 100 years return periods from regional frequency analysis of annual
798 maximum extreme precipitation events of 5 min. to 180 min. durations
799

Table 1: Climate stations (sites) and annual maximum extreme precipitation intensity used for regional analysis.

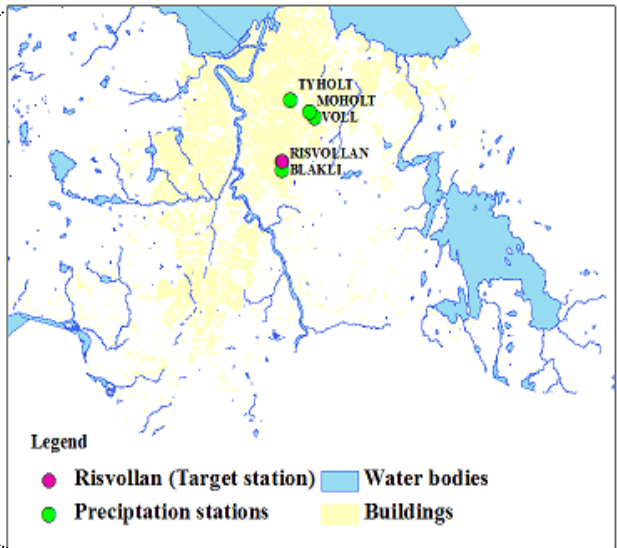
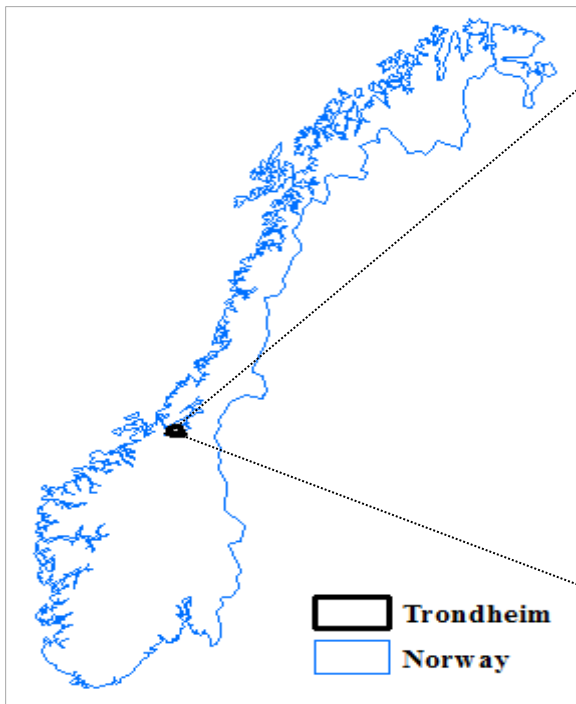
No.	Sites	Altitude, m amsl	Latitude (degree)	Longitude (degree)	Data range	No. of available data (years)	Mean annual total precipitation (mm)	Remarks
1	Risvollan	84	63.3987	10.4228	1987-2009	23	881	Target site (operational)
2	Moholt-Voll	127	63.4107	10.4535	1995-2009	13	855	Operational
3	Tyholt	113	63.4225	10.4303	1965-1993	25	740	Closed
4	Blakli	138	63.3960	10.4258	1974-1985	10	900	Closed
Total data used for regional analysis						71		

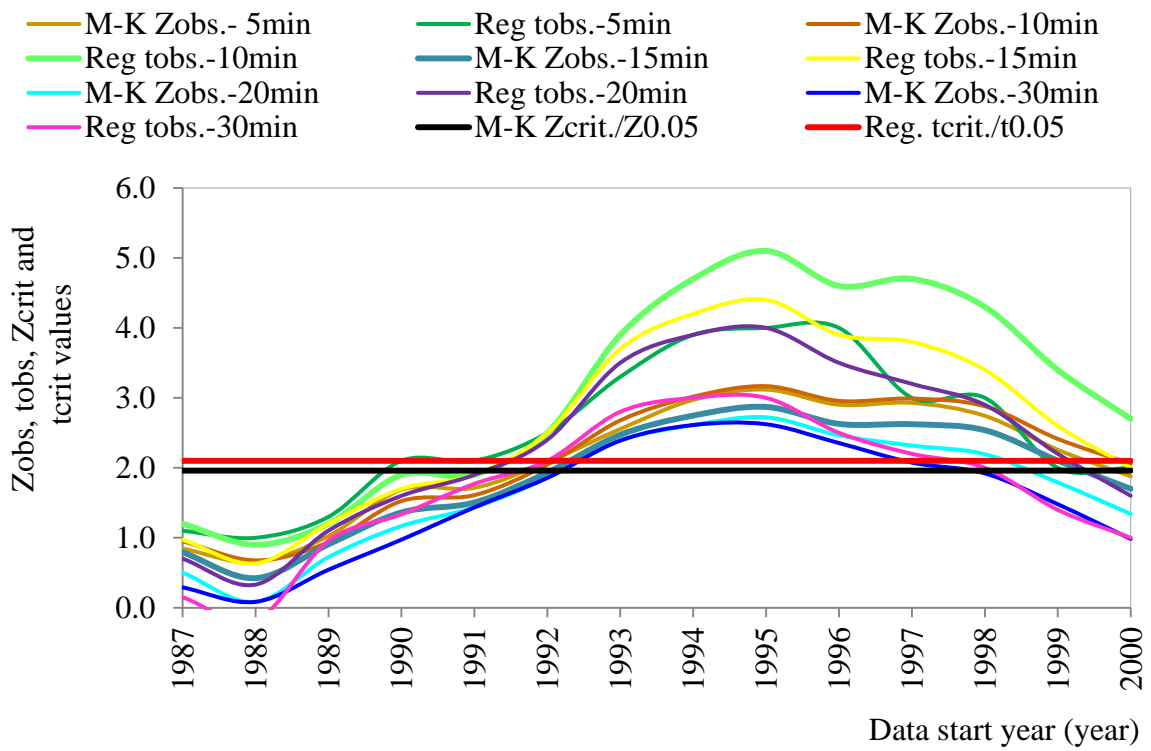
Table 2: Summary results for heterogeneity measures and goodness-of-fit measures (Z-statistics)

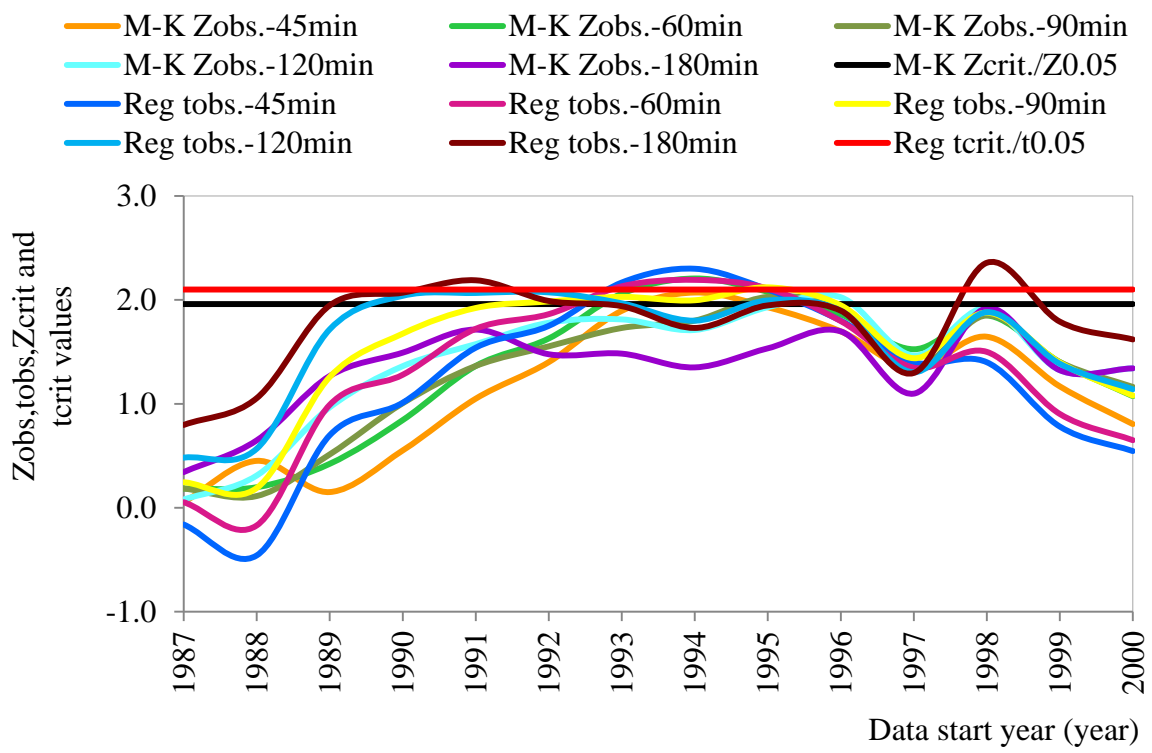
Durations (min.)	Heterogeneity measures			Z-statistics				"Best-fit" distribution
	H ₁	H ₂	H ₃	GLO	GEV	PIII	GPAR	
5	-1	-0.45	0.15	1.33	0.69	-0.04	-0.87	PIII
10	0.21	0.17	-0.58	3.26	2.33	1.88	0.28	GPAR
15	-0.17	-0.07	-0.39	4.31	3.31	2.96	1.17	GPAR
20	0.11	-0.04	0.23	4.2	3.26	2.83	1.2	GPAR
30	0.37	-1.18	-0.74	3.37	2.48	1.95	0.5	GPAR
45	-0.83	-1.3	-0.39	1.6	0.82	0.28	-0.95	PIII
60	-1.75	-1.44	-0.75	0.24	-0.48	-0.9	-2.09	GLO
90	-0.61	-1.81	-1.57	0.26	-0.47	-0.89	-2.1	GLO
120	0.31	-1.51	-0.29	2.01	1.08	0.73	-0.93	PIII
180	1.22	-1.25	-1.29	0.06	-0.73	-1	-2.44	GLO

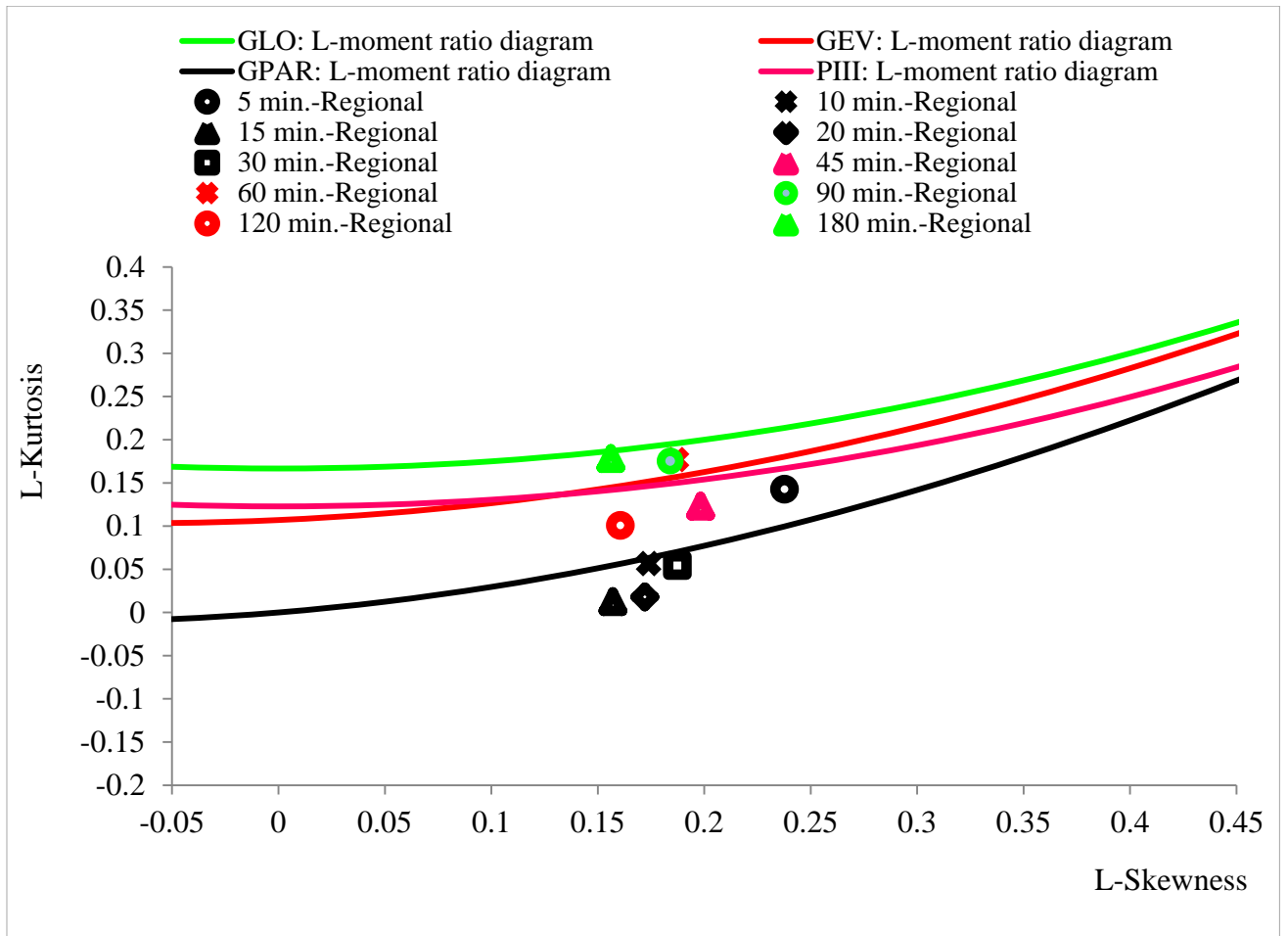
Table 3: Differences in percentages (%) for the lower and upper confidence levels estimated quantiles and the existing IDF curves from the estimated precipitation intensity quantiles from regional frequency analysis for a target site (Risvollan).

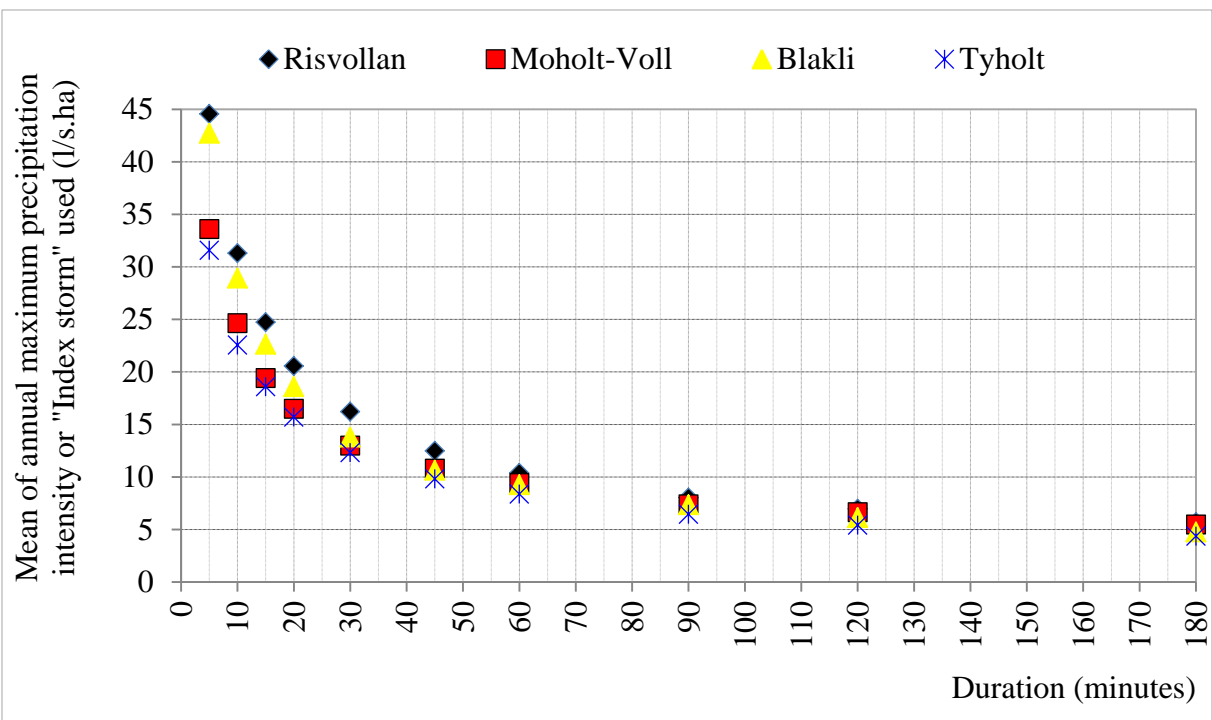
Return period (years)	Quantiles	Durations (min.)									
		5	10	15	20	30	45	60	90	120	180
2	95% LCL	-29.1	-28.1	-32.9	-31.4	-27.8	-30.7	-27.8	-26.3	-24.2	-25.1
	95% UCL	+25.1	+23.2	+23.0	+21.7	+19.7	+14.7	+9.6	+6.3	+6.9	0.0
	Existing IDF	+25.8	+23.4	+12.8	+16.4	+16.6	+9.1	+1.9	+8.7	+8.2	+12.0
5	95% LCL	-23.1	-21.0	-20.8	-22.1	-20.3	-19.4	-20.7	-17.1	-16.5	-17.8
	95% UCL	+24.7	+23.6	+23.3	+21.8	+21.7	+19.1	+15.3	+14.9	+12.2	+6.3
	Existing IDF	-1.1	-3.6	-4.9	+0.2	+7.0	-13.3	-16.7	-11.9	-11.0	+0.4
10	95% LCL	-28.7	-19.6	-17.1	-18.5	-18.0	-18.1	-18.1	-12.5	-17.5	-13.7
	95% UCL	+25.0	+22.2	+21.3	+19.9	+21.2	+20.2	+18.3	+19.0	+12.8	+10.6
	Existing IDF	-6.4	-8.5	-6.5	-1.6	+6.9	-20.4	-25.5	-20.8	-15.2	-6.0
20	95% LCL	-35.8	-21.0	-16.7	-16.9	-19.9	-19.0	-17.1	-11.3	-19.4	-11.6
	95% UCL	+24.5	+24.4	+20.1	+19.8	+23.4	+21.1	+20.5	+21.3	+13.3	+14.8
	Existing IDF	-8.9	-9.0	-4.4	+0.2	+9.7	-24.1	-31.4	-26.9	-17.9	-10.4
50	95% LCL	-42.4	-27.5	-21.4	-21.5	-26.7	-23.9	-23.0	-16.6	-21.9	-14.7
	95% UCL	+27.5	+27.2	+22.7	+23.6	+26.6	+20.4	+21.9	+22.8	+15.9	+19.7
	Existing IDF	-12.9	-6.1	+1.3	+5.6	+16.2	-25.9	-37.0	-32.0	-22.0	-15.0
100	95% LCL	-43.0	-36.5	-27.7	-26.7	-34.8	-30.3	-31.8	-24.3	-21.1	-19.3
	95% UCL	+31.1	+29.3	+24.0	+25.7	+29.3	+19.6	+23.4	+22.6	+19.6	+22.2
	Existing IDF	-18.3	-2.4	+7.1	+11.0	+22.4	-26.0	-40.0	-34.6	-26.0	-17.4

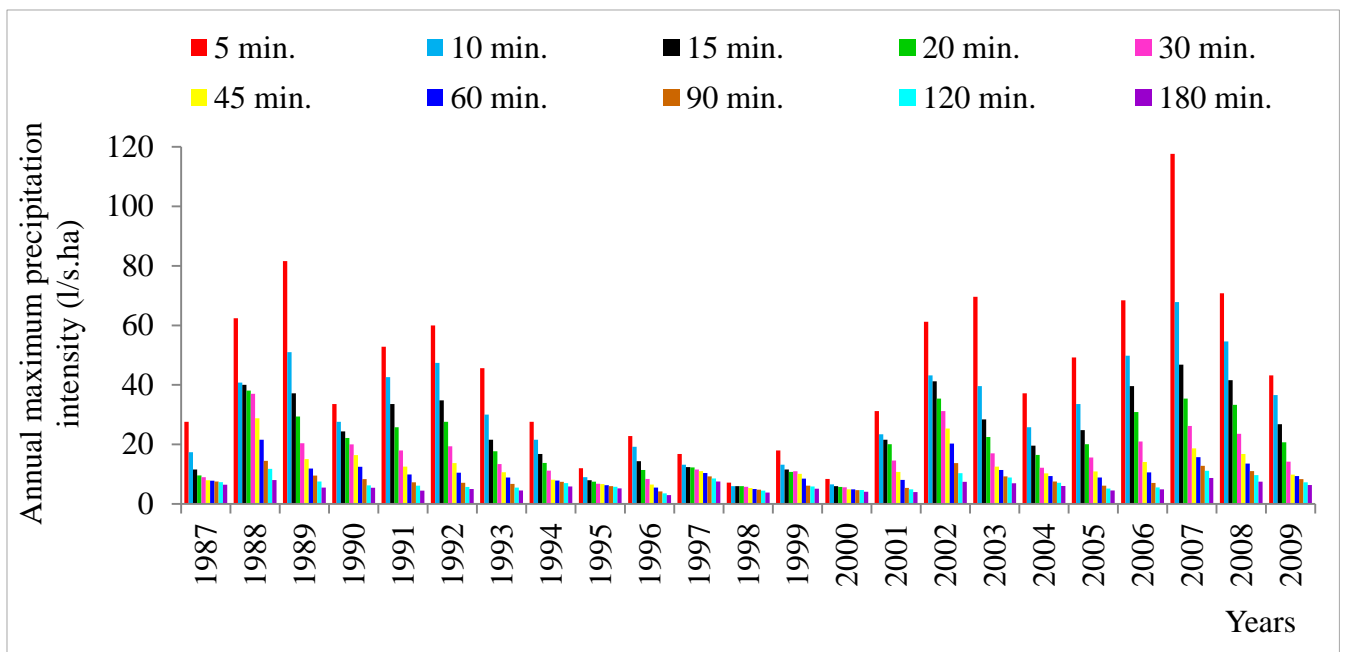


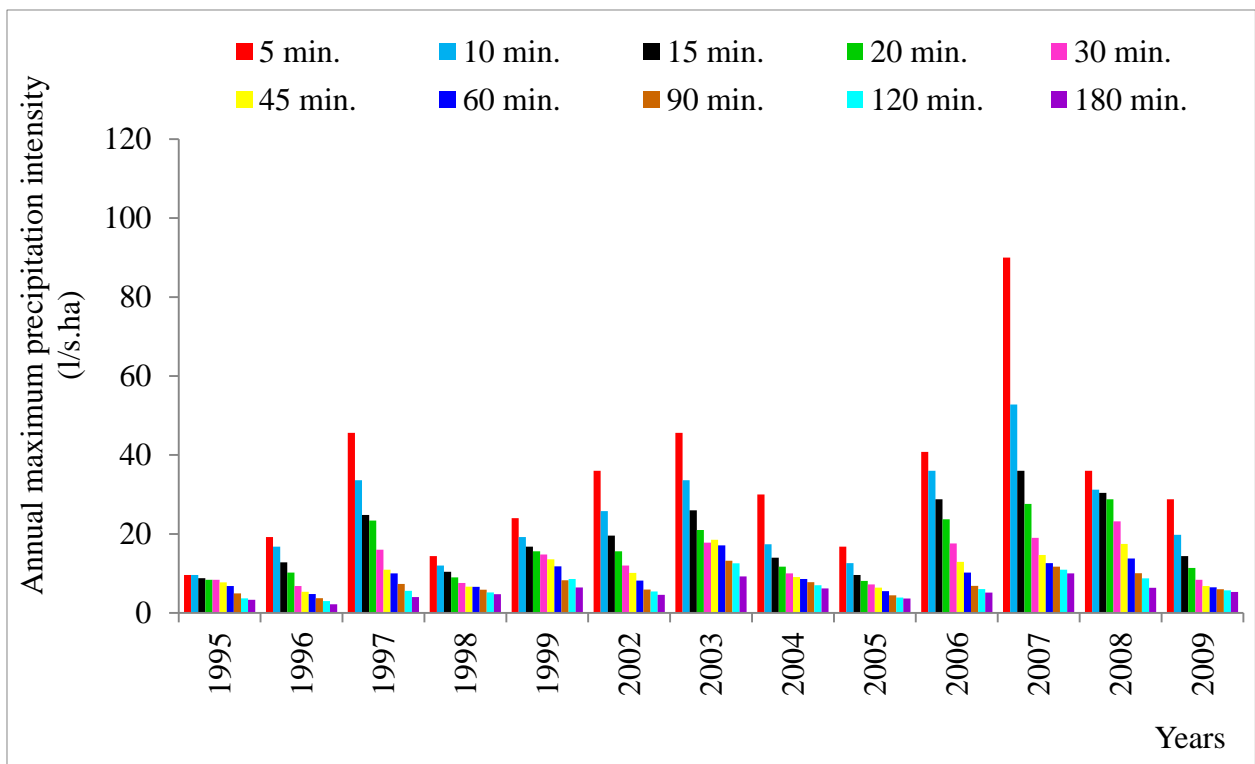


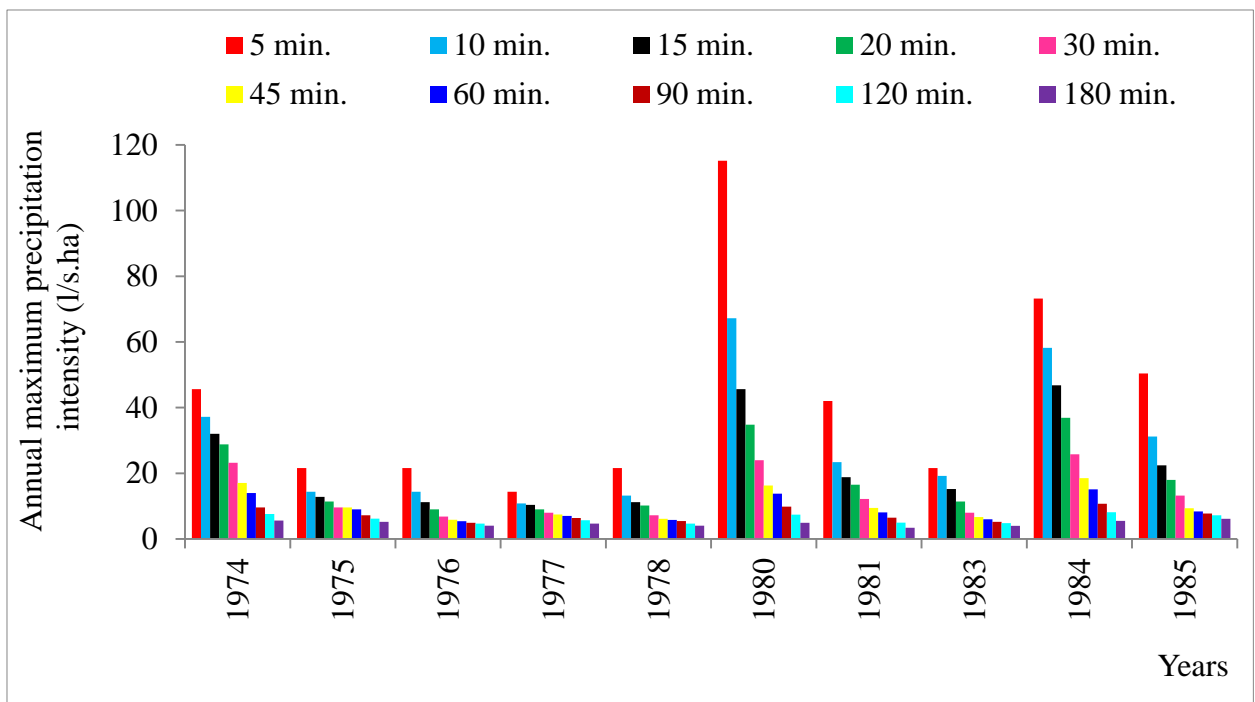


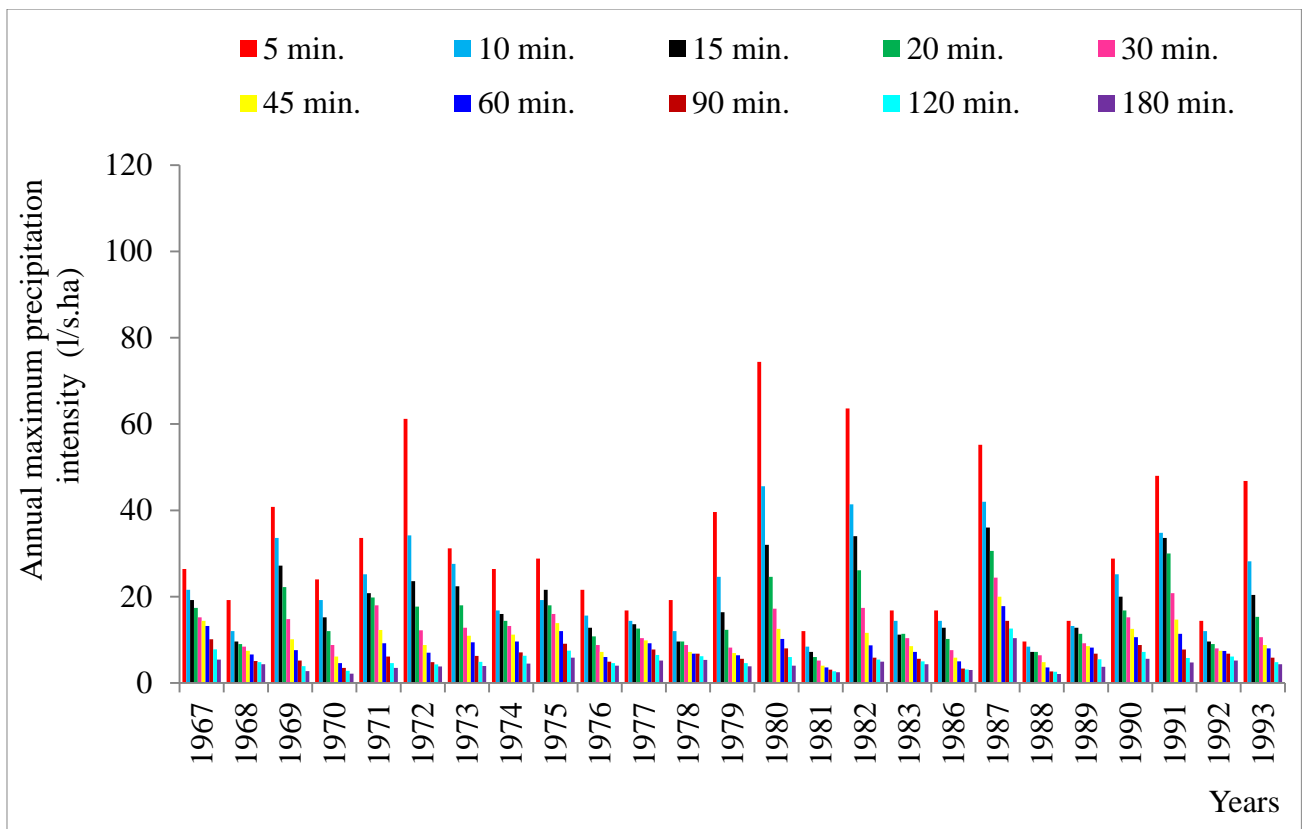


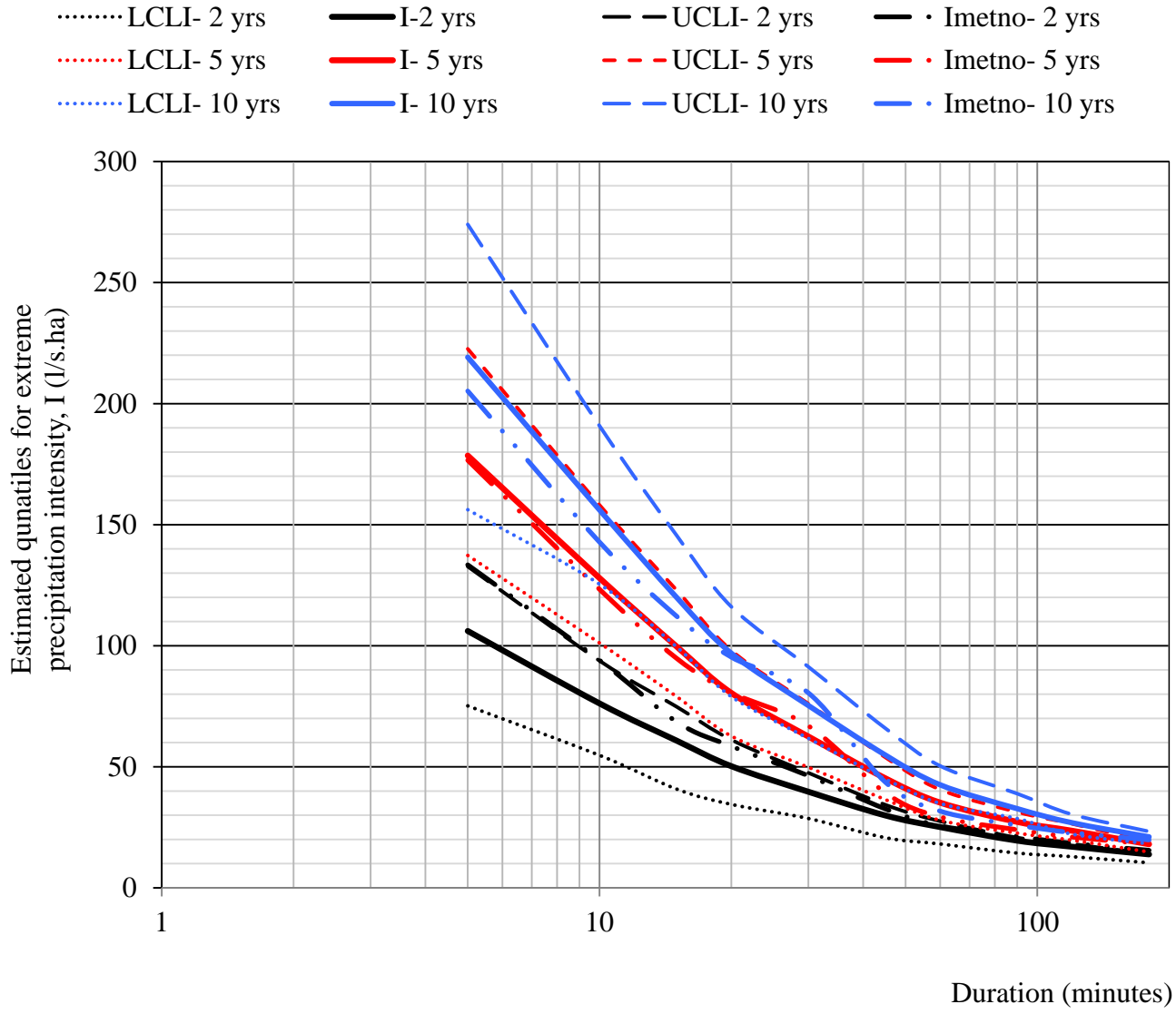


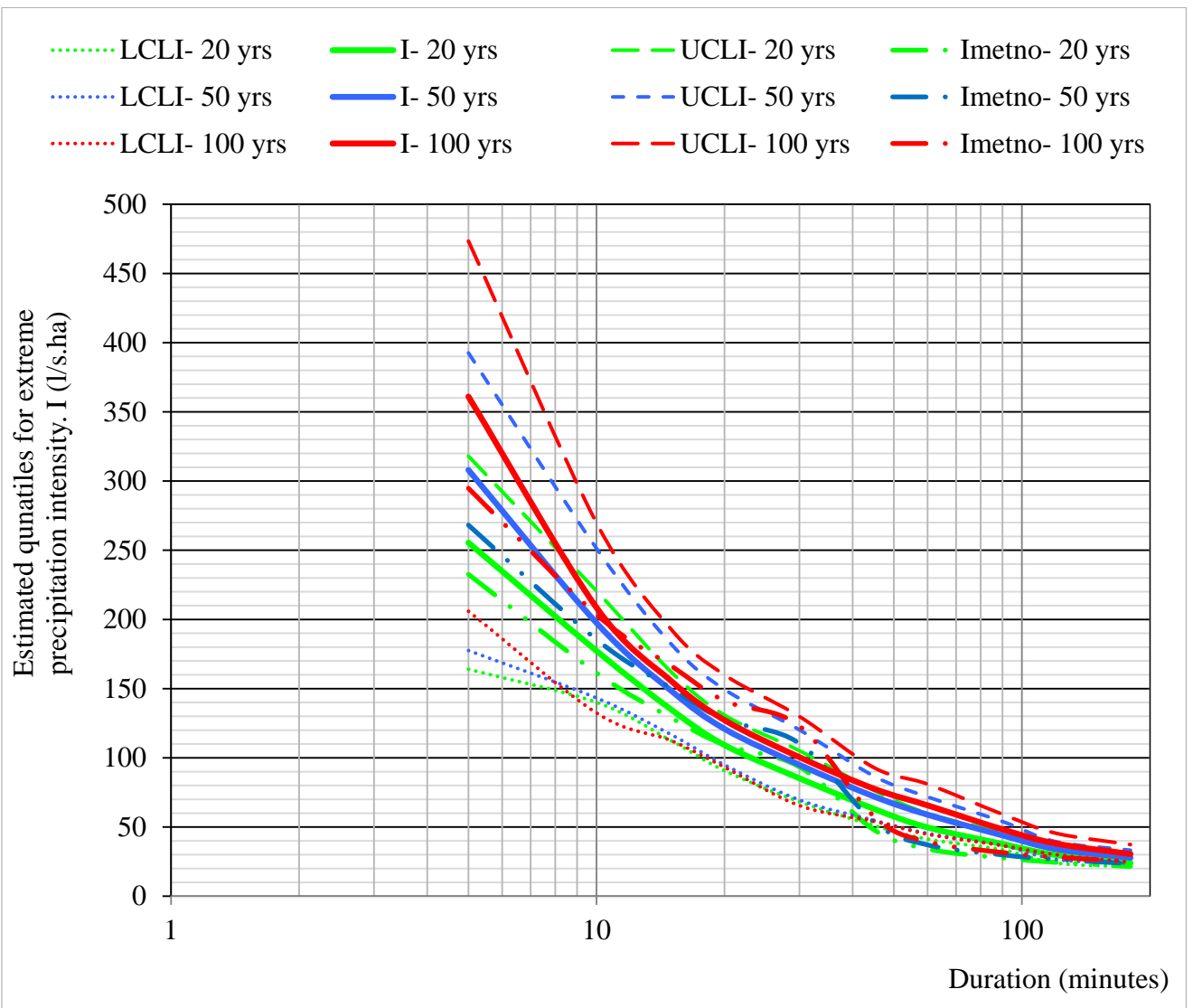












Appendix A: Probability density functions (PDF), cumulative distribution functions (CDF) and quantile functions (QF) for some statistical distributions (Hosking & Wallis, 1997).

Distributions	$f_X(x)$ or PDF	$F_X(x)$ or CDF	$x(F)$ or QF
GEV	$\frac{1}{\alpha} e^{-(1-k)y - e^{-y}}$ $y = -k^{-1} \ln \left\{ 1 - k \left(\frac{x - \xi}{\alpha} \right) \right\}$	$e^{-e^{-y}}$	$\xi + \frac{\alpha}{k} \left\{ 1 - (-\ln F)^k \right\}$
Pearson Type III	$\frac{1}{\beta \Gamma(\alpha)} \left(\frac{x - \xi}{\beta} \right)^{\alpha-1} e^{-\left(\frac{x - \xi}{\beta} \right)}$	$\frac{1}{\Gamma(\alpha)} \int_0^{\left(\frac{x - \xi}{\beta} \right)} u^{\alpha-1} e^{-u} du$	No explicit analytical form: Approximation by Wilson-Hilferty Transformation
Kappa	$\frac{1}{\alpha} \left\{ 1 - \frac{k}{\alpha} (x - \xi) \right\}^{\frac{1}{k}-1} \{F(x)\}^{1-h}$	$\left[1 - h \left\{ 1 - \frac{k}{\alpha} (x - \xi) \right\}^{\frac{1}{k}} \right]$	$\xi + \frac{\alpha}{k} \left\{ 1 - \left(\frac{1 - F^h}{h} \right)^k \right\}$
Wakeby	No explicit analytical form	No explicit analytical form	$\xi + \frac{\alpha}{\beta} \left\{ 1 - (1-F)^\beta \right\} - \frac{\gamma}{\delta} \left\{ 1 - (1-F)^{-\delta} \right\}$
GLOG	$\frac{\alpha^{-1} e^{-(1-k)y}}{(1 + e^{-y})^2}$ $y = -k^{-1} \log \left[1 - k \left(\frac{x - \xi}{\alpha} \right) \right], \quad k \neq 0$ $y = \frac{(x - \xi)}{\alpha}, \quad k = 0$	$\frac{1}{1 + e^{-y}}$	$\xi + \frac{\alpha}{k} \left\{ 1 - \left(\frac{1 - F}{F} \right)^k \right\}, \quad k \neq 0$ $\xi - \alpha \log \left(\frac{1 - F}{F} \right), \quad k = 0$

GPAR	$\alpha^{-1} e^{-(1-k)y}$ $y = -k^{-1} \log \left[1 - k \frac{(x-\xi)}{\alpha} \right], \quad k \neq 0$ $y = \frac{(x-\xi)}{\alpha}, \quad k = 0$	$1 - e^{-y}$	$\xi + \frac{\alpha}{k} \{1 - (1-F)^k\}, \quad k \neq 0$ $\xi - \alpha \log(1-F), \quad k = 0$
------	--	--------------	--

Appendix B: Parameters for the statistical distributions in Appendix A (Hosking & Wallis, 1997).

Distributions	Parameters			
	Location	Scale	Shape	
GEV	ξ	α	k	
Pearson Type III	ξ	β	α	
Kappa	ξ	α	$k \& h$	
Wakeby	ξ			$\alpha, \beta, \gamma \& \delta$
GLOG	ξ	α	k	
GPAR	ξ	α	k	